On the Diradical Character of Neutral Heteroleptic Bis(1,2-dithiolene) Metal Complexes: Case Study of [Pd(Me$_2$timdt)(mnt)] (Me$_2$timdt = 1,3-dimethyl-2,4,5-trithioxoimidazolidine; mnt^{2-} = 1,2-dicyano-1,2-ethylenedithiolate).

M. Carla Aragoni, Claudia Caltagirone, Vito Lippolis, Enrico Podda, Alexandra M. Z. Slawin, J. Derek Woollins, Anna Pintus,* and Massimiliano Arca*

KEYWORDS *1,2-Dithiolene, palladium, DFT, push-pull, broken-symmetry, NLO*

ABSTRACT: The reaction of the bis(1,2-ditiolene) complex [Pd(Me$_2$timdt)$_2$] (**1**; Me$_2$timdt$^{\bullet-}$ = monoreduced 1,3-dimethyl-2,4,5-trithioxoimidazolidine) with Br$_2$ yielded the complex [Pd(Me$_2$timdt)Br$_2$] (**2**), which was reacted with Na$_2$mnt (mnt^{2-} = 1,2-dicyano-1,2-ethylenedithiolate) to give the neutral mixed-ligand complex [Pd(Me$_2$timdt)(mnt)] (**3**). Complex **3** shows an intense solvatochromic near-infrared (NIR) absorption band falling between 955 nm in DMF and 1060 nm in CHCl$_3$ (ε = 10700 M^{-1} cm^{-1} in CHCl$_3$). DFT calculations were used to elucidate the electronic structure of complex **3**, and to compare it with those of the corresponding homoleptic complexes **1** and [Pd(mnt)$_2$] (**4**). An in-depth comparison of calculated and experimental structural and vis–NIR spectroscopic properties, supported by IEF-PCM TD-DFT and NBO calculations, clearly points to a description of **3** as a dithione-dithiolato complex. For the first time, a Broken-Symmetry (BS) procedure for the evaluation of the singlet diradical character (DC) of heteroleptic bis(1,2-dithiolene) complexes has been developed and applied to complex **3**. The DC, predominant for **1** (n_{DC} = 55.4%), provides a remarkable contribution to the electronic structures of the ground states of both **3** and **4**, showing a diradicaloid nature (n_{DC} = 24.9% and 27.5%, respectively). The computational approach developed here clearly shows that a rational design of the DC of bis(1,2-ditiolene) metal complexes, and hence their linear and nonlinear optical properties, can be achieved by a proper choice of the 1,2-dithiolene ligands based on their electronic structure.

INTRODUCTION

The interest of the scientific community towards bis(1,2-dithiolene) metal complexes has been continuously increasing during the past decades,[1,2,3,4,5,6] accompanied by a growing number of applications relying on the superconducting,[7,8,9,10,11,12] photoconducting,[13,14,15,16,17] magnetic, and linear and nonlinear optical properties[18,19,20,21,22] of this class of compounds. Bis(1,2-dithiolene) complexes $[M(R_2C_2S_2)_2]^{q-}$ of d^8 metal ions M^{x+}, such as Ni^{II}, Pd^{II}, Pt^{II}, and Au^{III}, feature peculiar properties,[5,23] such as molecular planarity and the ability to exist in well-defined oxidation states q typically ranging between x–4 and x–2,[24,25,26] also assuming fractional charges in non-integral oxidation state (NIOS) salts.[9,12] The redox non-innocence of the 1,2-dithiolene ligands (Scheme 1) renders it difficult to partition the charge of the complexes between the ligands L and the central metal ion M^{x+}.[27,28]

Scheme 1. Redox non-innocence of 1,2-dithiolene ligands: neutral 1,2-dithiete (a) and 1,2-dithione (b), radical 1,2-dithiolene anion (c), and dianionic ene-1,2-dithiolate (d)

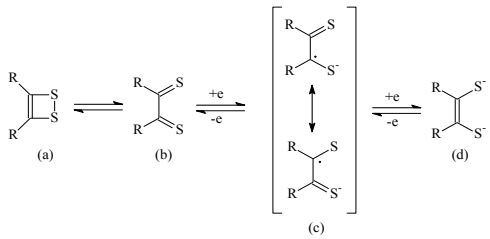

Scheme 2. Differently charged species and limit forms of bis(1,2-dithiolene) metal complexes (M = Ni, Pd, Pt; q = 0, 1, 2)

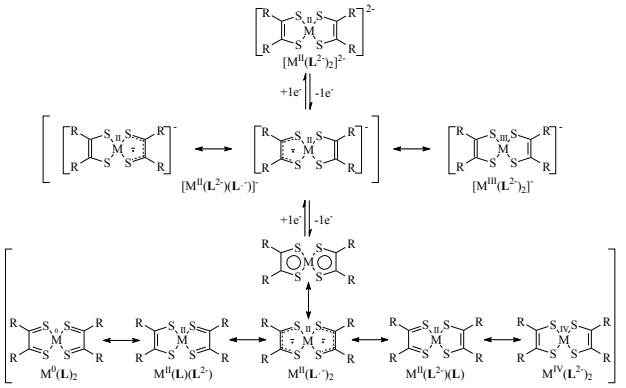

The typical redox steps accessible to bis(1,2-dithiolene) complexes of group 10 metals (M = Ni, Pd, and Pt) are summarized in Scheme 2. Dianionic bis(1,2-dithiolene) complexes $[ML_2]^{2-}$ are diamagnetic species, which can be isolated as stable anions in salts such as $(Ph_4P)_2[Ni(mnt)_2]$ (mnt^{2-} = maleonitrile-1,2-dithiolate, 1,2-dicyano-1,2-ethylenedithiolate).[29] These species are fully described as $[M^{II}(L^{2-})_2]^{2-}$ complexes, featuring the ene-1,2-dithiolato form L^{2-} of the ligands (d in Scheme 1). Paramagnetic monoanionic 1,2-dithiolene complexes $[ML_2]^{-}$ can be represented as $[M^{III}(L^{2-})_2]^{-}$

compounds[30,31] or by two limit forms showing a dianionic ligand $\mathbf{L}^{2-}$ (d in Scheme 1) and a monoanionic radical one $\mathbf{L}^{\bullet-}$ (c in Scheme 1), i.e. $[M^{II}(\mathbf{L}^{\bullet-})(\mathbf{L}^{2-})]^{-}$.[27] In diamagnetic neutral complexes $[M\mathbf{L}_2]$, the central metal ion can carry formal charges varying between 0 and +4, while the ligands can assume a neutral, monoanionic, or dianionic charge (Scheme 2), indicating a large degree of π-electron delocalization involving the metal as well as the **L** ligands (metalloaromaticity).[32] Spectroscopic and theoretical results suggest that the complexes are better described as formed by a metal dication M^{II}, whatever the charge on the complex.[27,33] Therefore, the oxidation/reduction steps leading from $[M\mathbf{L}_2]^{2-}$ to $[M\mathbf{L}_2]$ are mainly located on the ligands,[33,34,35] analogously to what reported for $[Au^{III}(Ar\text{-}edt)_2]^{0/-}$ complexes (Ar-edt^{2-} = arylethylene-1,2-dithiolate; Ar = phenyl, 2-naphthyl, 2-pyrenyl).[36] Hence, the neutral M^{II} complexes can be described as diamagnetic singlet species formed by two antiferromagnetically coupled monoanionic radical ligands, $[M^{II}(\mathbf{L}^{\bullet-})_2]$.[33,37] Indeed, neither the closed-shell (CS) restricted delocalized nor the localized singlet diradical descriptions represent reliably the ground state (GS) of neutral bis(1,2-dithiolene) complexes, so that an index n_{DC} of the diradical character (DC) can be calculated to evaluate the relative weight of the diradical singlet description.[37,38,39] Notably, different optical properties in the visible–near-infrared (vis–NIR) region are associated to the differently charged forms of bis(1,2-dithiolene) complexes (electrochromism).[16,40,56] Neutral complexes $[M\mathbf{L}_2]$ show a peculiar intense absorption in the region above 800 nm.[2,5,30] This band, attributed to a π–π^* HOMO→LUMO (H→L) one-electron excitation,[5,6] is shifted to lower energies and lowered in intensity in the corresponding monoreduced forms $[M\mathbf{L}_2]^{-}$,[41] while dianions $[M\mathbf{L}_2]^{2-}$ do not show any vis–NIR absorption. In this context, since few decades, some of the authors have been investigating the $[M(R'_2timdt)_2]^{q-}$ class of photoconducting[42,43,44] complexes ($R'_2timdt^{\bullet-}$ = monoreduced 1,3-disubstituted imidazoline-2,4,5-trithione; M = Ni, Pd, Pt; q = 0, 1, 2; Chart S1).[45,46,47,48,49,50,51,52] Neutral $[M(R'_2timdt)_2]$ complexes show a strikingly intense absorption at about 1000 nm (molar extinction coefficient ε as large as 120000 M^{-1} cm^{-1} in toluene),[48] whose energy can be fine-tuned by a proper choice of the metal M and the substituents R'.[46,48] The corresponding reduced forms show a NIR absorption falling at about 1450 nm for M = Ni and Pt, and at about 1700 nm for M = Pd.[51]

Mixed-ligand bis(1,2-dithiolene) complexes $[M(\mathbf{L})(\mathbf{L}')]$ are much less investigated than homoleptic ones,[48,53] and are often prepared by metathesis reactions.[54,55,56] The synthetic way of obtaining $[M(\mathbf{L})(\mathbf{L}')]$ complexes by replacement of halides in $M\mathbf{L}X_2$ complexes has been previously reported in few cases.[48] In these complexes, most often containing a Ni^{II} ion,[31,57,58,59,60,61] the most electron-withdrawing "pull" ligand **L** tends to assume an ene-1,2-dithiolate form $\mathbf{L}^{2-}$ (d in Scheme 1), with shorter C–C and longer C–S bond distances, while the other "push" ligand (**L'**), a 1,2-dithione form (b in Scheme 1), with longer C–C and shorter C–S distances, so that the complex is generally described as a dithione-dithiolato species $[M^{II}(\mathbf{L}^{2-})(\mathbf{L}')]$. The electronic structure of these complexes in their neutral state, reminding that of diimine-dichalcogenolato complexes,[62,63,64] shows the HOMO featuring a larger contribution from the "pull" ligand $\mathbf{L}^{2-}$ and the LUMO from the "push" ligand **L'**. The peculiar visible–near-IR (Vis–NIR) electron transition of the neutral species assumes a partial Charge-Transfer (CT) character from the 1,2-dithiolato $\mathbf{L}^{2-}$ ligand to the 1,2-dithione **L'** (LL'CT), testified by a remarkable negative solvatochromism of the resulting absorption band.[54] As compared to homoleptic complexes, the DC of heteroleptic bis(1,2-dithiolene) complexes has not been investigated, implicitly accepting that the GS configuration of these complexes is fully defined by the dithione-dithiolato CS description.[48] Nevertheless, it is conceivable that a continuous variation from ideally pure open-shell singlet diradicals $[M^{II}(\mathbf{L}^{\bullet-})(\mathbf{L}'^{\bullet-})]$ to CS dithione-dithiolato complexes $[M^{II}(\mathbf{L})(\mathbf{L}'^{2-})]$ occurs as the difference in the donor properties of the **L** and **L'** ligands increases. Therefore, we have considered as a case study the mixed-ligand 1,2-dithiolene Pd^{II} complex featuring the well-known mnt "pull" ligand coupled to the "push" ligand Me_2timdt. Herein, we report an experimental and theoretical investigation on the resulting complex $[Pd(Me_2timdt)(mnt)]$, compared with the relevant parent complexes $[Pd(Me_2timdt)_2]$ and $[Pd(mnt)_2]$, aimed at evaluating the role of the electronic structure of the ligands in tailoring the DC in homoleptic and heteroleptic bis(1,2-dithiolene) palladium complexes.

EXPERIMENTAL SECTION

Materials and Methods. Reagents were purchased from Honeywell, Alfa Aesar, and Sigma-Aldrich and used without further purification. Solvents (reagent grade) were purchased from Honeywell, VWR, and Merck and dried by using standard techniques when required. Manipulations were performed using standard Schlenk techniques under dry dinitrogen atmosphere. Elemental analyses were performed with a CHNS/O PE 2400 series II CHNS/O elemental analyzer (T = 925 °C). FT-IR spectra were recorded with a Thermo-Nicolet 5700 spectrometer at room temperature: KBr pellets with a KBr beam-splitter and KBr windows (4000–400 cm^{-1}, resolution 4 cm^{-1}) were used. Absorption spectra were recorded at 25 °C in a quartz cell of 10.00 mm optical path either with a Thermo Evolution 300 (190–1100 nm) spectrophotometer or an Agilent Cary 5000 UV–vis–NIR (190–2000 nm) dual-beam spectrophotometer. Absorption spectra were decomposed into their constituent Gaussian peaks using the Specpeak 2.0[65] and Fityk 1.3.1[66] programs. The Crystallographic Structural Database was accessed by using CCDC ConQuest 2020.1.[67]

X-ray Diffraction Measurements. Single-crystal X-ray diffraction data were collected with a Rigaku MM007/Mercury diffractometer with Mo-Kα radiation. The structure was solved by direct methods with SHELXS-97[68] and refined on F^2 by using SHELXL-97.[69]

Synthesis. 1,3-Dimethyl-2-thioxoimidazolidine-4,5-dione and complex **1** were prepared according to a previously reported procedure (yield 86%).[45,46,70]

*Synthesis of [Pd(Me₂timdt)Br₂] (**2**).* $[Pd(Me_2timdt)_2]$ (**1**; 35.4 mg; $7.27\cdot10^{-2}$ mmol) was reacted with an excess of molecular dibromine in an Aldrich pressure tube using 30 mL of a $CHCl_3/CH_3CN$ (2:1) solvent mixture. The glass vessel was heated to 130 °C for 15 min and slowly cooled to room temperature. The precipitate was filtered and washed with petroleum ether (brown solid; yield 32.1 mg, 97%). M. p. > 230 °C. FT-IR (4000–400 cm^{-1}): ν = 1477 (s), 1399 (s), 1360 (m), 1345 (m), 1291 (s), 1080 (s), 1032 (mw), 548 cm^{-1} (w). Elemental analysis calcd (%) for $C_5H_6Br_2N_2PdS_3$: C 14.10, H 0.76, N 8.11. Found: C 14.86, H 0.33, N 9.02.

*Synthesis of [Pd(Me₂timdt)(mnt)] (**3**).* Complex **2** (30.2 mg; $6.61\cdot10^{-2}$ mmol) and a molar excess of sodium 1,2-dicyano-ethylene-1,2-dithiolate (21.5 mg; 0.115 mmol) were suspended in CH_3CN (30 mL) in an Aldrich pressure tube. The mixture was heated to 130 °C for 30 min and slowly cooled to room temperature. The product was isolated as black needles by filtration, washed with water and dried under vacuum (yield 8.3 mg, 29%). M. p. > 230 °C. FT-IR (4000–400 cm^{-1}): ν = 2925 (w), 2204 (m), 1459 (m), 1397 (ms), 1285 (s),

Scheme 3. Reaction pathways for the synthesis of 3. i: Lawesson's reagent, refluxing toluene, N_2; ii: $PdCl_2$; iii: Br_2, $CHCl_3/CH_3CN$ 2:1, 130 °C; iv: Na_2mnt, CH_3CN, 130 °C

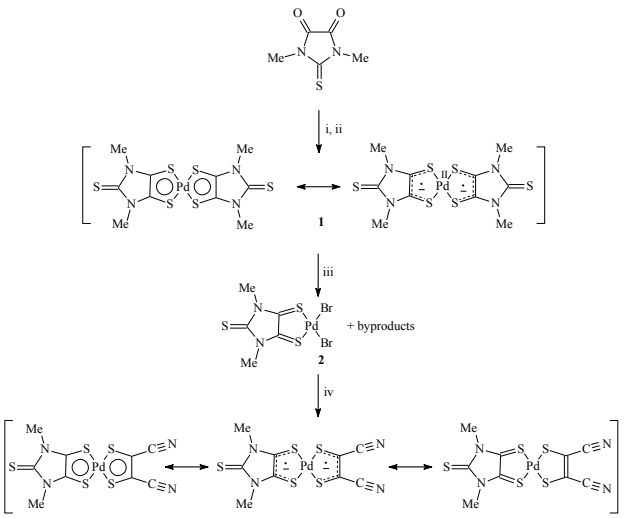

1150 (m), 1079 (ms), 864 (m), 551 (mw), 500 cm^{-1} (mw). Elemental analysis calcd (%) for $C_9H_6N_4PdS_5$: C 24.74, H 1.38, N 12.82. Found: C 24.68, H 0.45, N 13.07.

Theoretical Calculations. Quantum-chemical calculations were carried out on $[Pd(Me_2timdt)_2]^{q-}$ (**1**$^{q-}$; Chart S2 for q = 0), $[Pd(Me_2timdt)Br_2]$ (**2**; Chart S2), $[Pd(Me_2timdt)(mnt)]^{q-}$ (**3**$^{q-}$; q = 0, 1, 2; Chart S2 for q = 0), $[Pd(mnt)_2]^{q-}$ (**4**$^{q-}$; q = 0, 1, 2; Chart S2 for q = 0), [Pt(phen)(tdt)] (phen = 1,10-phenanthroline; tdt^{2-} = 3,4-toluenedithiolate; Chart S2),[71] $[Ni(bdt)_2]$ (bdt^{2-} = benzene-1,2-dithiolate)[33,37] and compounds $(Me_2timdt)_2$ (Chart S2), Li(R''$_2$timdt)·2THF (R'' = 2,6-diisopropylphenyl; **5**; Chart S2),[72,73] and $Me_2timdt(SPh)_2$ (**7**; Chart S2)[74] at the density functional theory (DFT)[75] level with the commercial suite Gaussian 16.[76] The computational setup was validated as previously described for the strictly related $[Ni(Me_2timdt)_2]$ complex and derivatives,[52] and it kept into account three hybrid functionals (B3LYP,[77] mPW1PW,[78] and PBE0[79]) and six basis sets with Relativistic Effective Core Potentials (RECPs)[80,81] for the central metal ion [LANL08(f),[82] SBKJC,[83] Stuttgart 1997 RC,[84] CRENBL,[85] LANL2DZ,[86] and LANL2TZ[82]]. DFT calculations were eventually carried out with the hybrid mPW1PW functional,[78] including a modified Perdew and Wang (PW) exchange functional coupled with the PW correlation functional.[87,88] Schäfer, Horn, and Ahlrichs double-ζ plus polarization (pVDZ)[89] all-electron basis sets for light atomic species (C, H, N, S), and CRENBL basis sets[85] with relativistic effective core potentials (RECP) for heavier atomic species (Pd and Br) were used. Basis sets and RECPs were obtained from Basis Set Exchange and Basis Set EMSL Library.[90] Dianionic bis(1,2-dithiolene) complex species were modeled according to a closed-shell (CS) restricted description (RDFT), monoanionic paramagnetic species within an unrestricted formalism (UDFT), while neutral species were investigated (a) in their triplet ground state ($2S + 1 = 3$, two unpaired electrons), (b) in the closed-shell singlet state ($2S + 1 = 1$), or (c) as antiferromagnetically coupled singlet diradicals in a broken-symmetry (DFT-BS) approach. The latter description was obtained starting from the triplet state, by attributing the two antiparallel electrons to the two 1,2-dithiolene ligands (Chart S3 in SI). The BS electron density guess was obtained through a fragment approach (*guess=fragment*=3, the three fragments being the Pd^{II} ion and the two monoanionic 1,2-dithiolene radical ligands), eventually allowing to optimize (*opt*) the geometry of the complex (BS1 solution). Finally, only in the case of **1**, the guess of the electron density of the lowest BS singlet excited state (ES) was used to reoptimize the geometry of the GS electronic structure of the complex, obtaining an alternative minimum for the BS GS configuration (BS2), degenerate with respect to the BS1 description ($|\Delta\mathcal{E}_{BS2-BS1}| \approx 8{\cdot}10^{-4}$ Hartree). For all compounds, tight SCF convergence criteria and fine numerical integration grids (*grid=ultrafine*) were used. In order to evaluate the singlet diradical contribution to the GS in the BS approach, the differences between the total electronic energy of the singlet state ($\mathcal{E}_S$), the BS-singlet ($\mathcal{E}_{BS}$), and the triplet ($\mathcal{E}_T$) states were considered:[38,91,92]

$$\mathcal{E}_1 = \mathcal{E}_{BS} - \mathcal{E}_S \qquad \text{eq 1}$$

$$\mathcal{E}_2 = \mathcal{E}_T - \mathcal{E}_S \qquad \text{eq 2}$$

The effective electron exchange integrals J_{ab}[93] were calculated as follows:

$$J_{ab} = \frac{\mathcal{E}_1 - \mathcal{E}_2}{\langle S^2\rangle_T - \langle S^2\rangle_{BS}} = \frac{\mathcal{E}_{BS} - \mathcal{E}_T}{\langle S^2\rangle_T - \langle S^2\rangle_{BS}} \qquad \text{eq 3}$$

where $\langle S^2\rangle_T$ and $\langle S^2\rangle_{BS}$ represent the spin expectation values[94,95] determined at the optimized geometry for the triplet and broken-symmetry GSs, respectively, after verification of the wavefunction stability (*stable=opt*). The singlet-triplet energy gap $\Delta\mathcal{E}_{ST}^{SC} = \mathcal{E}_S^{SC} - \mathcal{E}_T$, accounting for the effect of spin contamination to the energy of the singlet GS,[95] corresponding to a mixing of the singlet and triple state, was calculated as:

$$\Delta\mathcal{E}_{ST}^{SC} = \Delta\mathcal{E}_{ST}\frac{\langle S^2\rangle_T}{\langle S^2\rangle_T - \langle S^2\rangle_{BS}}$$

Therefore, the $\mathcal{E}_S^{SC}$ value was obtained:

$$\mathcal{E}_S^{SC} = \mathcal{E}_T + \Delta\mathcal{E}_{ST}\frac{\langle S^2\rangle_T}{\langle S^2\rangle_T - \langle S^2\rangle_{BS}} \qquad \text{eq 4}$$

The diradical character n_{DC} index can be directly calculated from $\langle S^2\rangle_{BS}$:[17,37]

$$n_{DC} = 1 - \sqrt{1 - \langle S^2\rangle_{BS}} \qquad \text{eq 5}$$

A complete natural population analysis (NPA) was carried out with a Natural Bonding Orbital (NBO)[96] partitioning scheme (*pop=nboread*, with *boao* and *bndidx* keywords in the NBO section of the input file) in order to investigate the charge distributions and Wiberg bond indexes.[97] Absorption vertical transition energies and oscillator strengths were calculated at time-dependent (TD) DFT level.[98,99] TD-DFT calculations were carried out at the optimized geometry in the gas phase and in a selection of solvents ($CHCl_3$, CH_2Cl_2, DMF, THF, acetonitrile), implicitly taken into account by means of the polarizable continuum model in its integral equation formalism (IEF-PCM),[100] describing the cavity of the complexes within the reaction field (SCRF) through a set of overlapping spheres. Oscillator strength values calculated at TD-DFT level along with experimental FWHM values of the NIR band were used to evaluate the molar extinction coefficients ε.[101] Experimental FWHMs on an energy scale (eV) were evaluated from the corresponding values w determined in nm from the experimental NIR spectra.

$$W = 10^7\frac{w}{\lambda_0{}^2 - \frac{1}{4}w^2}$$

The one-photon absorption oscillator strength f_{0n} for each transition $0 \rightarrow n$ is:[102]

$$f_{0n} = \frac{8\pi^2 m_e \nu_{0n} |\mu_{0n}|^2}{3e^2 h}$$

where m_e and e are the mass and the charge of the electron, ν_{0n} is the frequency (s^{-1}) of the transition between the states 0 and n, μ_{0n} is the transition dipole moment, and h is Planck's constant. f_{0n} is related to the experimental intensity of each absorption band:

$$f_{0n} = 4.32 \cdot 10^{-9} \int \varepsilon(\varpi) d\varpi$$

where ε is the molar extinction coefficient (M^{-1} cm^{-1}) and ϖ is the frequency (cm^{-1}). By adopting Gaussian curve-shapes for the absorption bands:

$$f_{0n} = 4.32 \cdot 10^{-9} \varepsilon \int e^{-(\Delta\varpi/\theta)^2} d\varpi$$

$$f_{0n} = 4.32 \cdot 10^{-9} \sqrt{\pi} \varepsilon \theta$$

where the width parameter θ is related to W by:

$$\theta = \frac{W}{2\sqrt{\ln(2)}}$$

Therefore, the equation:

$$\varepsilon_{calc} = \frac{2\sqrt{\ln(2)}}{4.32 \cdot 10^{-9}\sqrt{\pi}} \cdot \frac{f_{0n}}{W} \qquad \text{eq 6}$$

allows evaluating the molar extinction coefficients of the NIR transition at TD-DFT level. Calculated molar extinction coefficients were scaled on experimental available data to give a corrected $\varepsilon_{calc}^{corr}$ value.

The nature of the minima of each structure optimized at DFT and DFT-BS level was verified by harmonic frequency calculations (*freq=raman*), including the determination of thermochemistry parameters [zero-point energy (ZPE) corrections and thermal corrections to enthalpy and Gibbs free energy] and the calculation of FT-Raman frequencies. Gibbs free energies were used to calculate absolute reduction potentials at 298 K (E_{Abs}^{298K}) according to the following equation:[103,104,105,106]

$$E_{Abs}^{298K} = \frac{\Delta G_{neutral}^{298K} - \Delta G_{anion}^{298K} - \Delta G_e^{\circ}}{F} \qquad \text{eq 7}$$

where $\Delta G_{neutral}^{298K}$ and ΔG_{anion}^{298K} are the free energy values calculated at 298 K and $\Delta G_e^{\circ}/F$ represents the potential of the free electron (–0.03766 eV at 298 K; $\Delta G_{neutral}^{298K}$ is calculated on the most stable neutral form).[107] E_{Abs}^{298K} were also referred to the Fc^+/Fc couple, taken into account at the same level of theory.

The total static (i.e. under zero frequency)[108] second-order (quadratic) hyperpolarizability (the first hyperpolarizability)[109] β_{tot} was calculated as previously described.[110]

Throughout all this work, molecules in their optimized standard orientation were rotated in order to align the main symmetry axis (bisecting C–C 1,2-dithiolene bonds and passing through the central metal ion) with the z axis and lie on the yz plane. Molden 6.2[111] and GaussView 6.0.16[112] were used to analyze Kohn-Sham (KS) molecular orbital (MO) compositions and energies. GaussSum 3.0[113] and Chemissian 4.54[114] were used to evaluate the atomic orbital contributions to KS-MOs and to analyze TD-DFT data.

RESULTS AND DISCUSSION

Synthesis. The synthesis of $[Pd(R'_2timdt)_2]$ neutral complexes can be achieved by direct sulfuration with Lawesson's reagent [2,4-bis(4-methoxyphenyl)-1,3,2,4-dithiadiphosphetane-2,4-disulfide][115] of the corresponding 1,3-disubstituted 2-thioxoimidazolidine-4,5-diones, followed by addition of $PdCl_2$ (reactions i and ii in Scheme 3).[45,46] The reaction of a suspension of $[Pd(Me_2timdt)_2]$ (**1**) in a 2:1 $CHCl_3/CH_3CN$ solvent mixture with a molar excess of molecular dibromine in a high pressure tube at 130 °C yielded the neutral complex $[Pd(Me_2timdt)Br_2]$ (**2**; reaction iii in Scheme 3), that was successively made to react with sodium 1,2-dicyanoethylene-1,2-dithiolate (Na_2mnt) in $CHCl_3$ at 130 °C to give the mixed-ligand neutral complex $[Pd(Me_2timdt)(mnt)]$ (**3**; reaction iv in Scheme 3).

X-ray Diffraction Studies. Tiny needle crystals of **3**, suitable for a structural characterization by X-ray diffraction analysis (Figure 1; Tables S1–S6, Figures S1 and S2), were isolated from the reaction mixture. The structural features of **3** (Figure 1) closely resemble those determined previously for $[Pd(Et_2timdt)(mnt)]$.[48] The molecule is planar but for the methyl substituents, with the central Pd ion coordinated by the two 1,2-dithiolene ligands in a pseudo square-planar fashion, with unbalanced Pd–S bond distances [Pd–S(1), 2.314(2); Pd–S(4), 2.258(2) Å]. The $C(1)–C(1)^i$ bond length within the Me_2timdt ligand [1.454(16)] is longer than those previously reported for $[Pd(Et_2timdt)_2]$ [1.397(9) Å],[45] while the $C(1)–S(1)/C(1)^i–S(1)^i$ distances [1.660(8) Å] are shorter [corresponding averaged value in $[Pd(Et_2timdt)_2]$ = 1.689(8) Å], suggesting a larger character of ene-1,2-dithiolate of the Me_2timdt ligand **3** as compared to the Et_2timdt ligands in $[Pd(Et_2timdt)_2]$. When comparing the two C_2S_2Pd metallacycles in **3**, the $C(4)–C(4)^i$ length in the mnt unit [1.364(16) Å] is shorter than that in the Me_2timdt one, while the C–S distances are longer in the mnt ligand [C(4)–S(4) 1.724(8) Å]. The C–C distance in the Me_2timdt ligand of **3** [1.454(16) Å] is intermediate between the corresponding distance in $[Pd(Et_2timdt)Br_2]$ [1.474(10) Å; Chart S2],[48] featuring an authentic neutral Et_2timdt ligand, and that of $Li(R''_2timdt)\cdot 2THF$ (R'' = 2,6-diisopropylphenyl) (**5**; Chart S2) [1.417(4) Å], featuring the $R''_2timdt^{\bullet-}$ radical monoanion.[72,73] Analogously, the $C(4)–C(4)^i$ distance in **3** [1.364(16) Å] is shorter than that found in $[Pd(mnt)_2]$ [**4**; 1.39(2) Å; Chart S2][116] and the average value for $\mathbf{4}^-$ monoanions [1.377(24) Å],[117] but slightly larger than the average value found in salts of the complex $\mathbf{4}^{2-}$ [1.359(19) Å].[118] This suggests that the Me_2timdt ligand in **3** should be considered to carry a partial negative charge, and that the GS of **3** should include a partial DC. The unit cell contains pairs ($Z = 2$) of symmetry-related complex molecules, each forming slipped stacks along the a vector (Figures S1 and S2 in SI) with an interplanar distance of 3.619 Å, very close to that featured by the stacks found in the crystal structure of $[Pd(Et_2timdt)_2]$[45] (3.6 Å). Along the stacks, the terminal thione groups of the Me_2timdt ligands weakly interact with the π-system of the imidazoline ring [$C(1)^{ii/iii}–S(2)$ 3.420 Å; ^{ii} = –1+x, y, z; ^{iii} = –1+x, 1/2-y, z; Figure S1]. Weak contacts between the methyl substituents at the Me_2timdt ligands and the terminal N-atoms of the mnt ligands [$H(3A)\cdots N(5)^{iv}$ 2.644 Å; ^{iv} = –1+x, y, 1+z] are responsible for the interactions between adjacent stacks aligned along the c direction. Notably, the crystal packing is sensibly different from that found in $[Pd(Et_2timdt)(mnt)]$, where the complex molecules are stacked in an alternate head-to-tail disposition allowing for shorter interplanar distances (3.570 Å).[48]

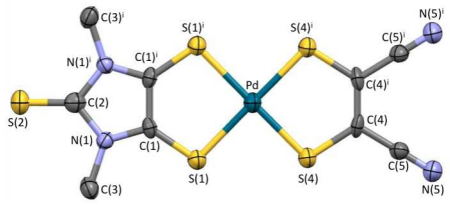

Figure 1. ORTEP view of complex **3** with the adopted labelling scheme. Selected bond distances and angles: Pd–S(1) 2.314(2), C(1)–S(1) 1.660(8), C(1)–C(1)^{i} 1.454(16), C(1)–N(1) 1.342(9), N(1)–C(3) 1.454(10), N(1)–C(2) 1.401(10), C(2)–S(2) 1.603(13), Pd–S(4) 2.258(2), C(4)–S(4) 1.724(8), C(4)–C(4)^{i} 1.364(16), C(4)–C(5) 1.423(11), N(5)–C(5) 1.139(10) Å; S(1)–Pd–(S1)^{i} 91.53(12); S(1)–Pd–(S1)^{i} 90.61(12); S(1)–Pd–S(4) 88.92(8); C(1)–S(1)–Pd–S(4) 179.6(2), S(1)–Pd–S(4)–C(4) 177.3(2) °. Displacement ellipsoids are drawn at a 30% probability level. Hydrogen atoms were omitted for clarity. Symmetry operation: ^{i} = x, 1/2–y, z.

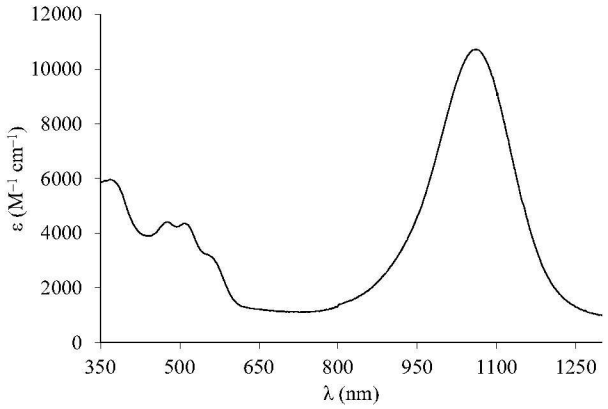

Figure 2. UV–vis–NIR absorption spectrum (350–1300 nm) of **3** in $CHCl_3$ solution.

2.3 Absorption Spectroscopy. Neutral [Pd(R'$_2$timdt)$_2$] bis(1,2-dithiolene) complexes featuring alkyl R substituents show a peculiar intense NIR absorption falling at about 1010 nm, with molar extinction coefficients ε as high as 70000 M^{-1} cm^{-1} in CH_2Cl_2.[45,46] The UV–vis–NIR absorption spectrum of a CH_2Cl_2 solution of **1** shows a NIR absorption maximum falling at 1008 nm [full width at half maximum (FWHM) w = 131 nm; Figure S3]. Notably, the NIR peak shows at least three Gaussian components (λ_1 = 1004.8 nm, w_1 = 121.9 nm, integral ratio 74.5%; λ_2 = 890.3 nm, w_2 = 93.5 nm, 6.6%; λ_3 = 1120.2 nm, w_3 = 155.4 nm, 18.9%; Figure S3),[65] in agreement with the spectral decomposition reported for [Pd(2,4-^{t}Bu$_2$C$_6$H$_2$S$_2$)$_2$], for which a series of *d*–*d* transitions with different spin coupling to the open-shell ligands were envisaged.[33] Complex **3** shows a well-defined intense NIR peak at 1060 nm in $CHCl_3$ (ε = 10700 M^{-1} cm^{-1}; Figure 2), in perfect agreement with the spectral features shown by [Pd(Et$_2$timdt)(mnt)] in the same solvent (λ_{max} = 1061 nm, ε = 12500 M^{-1} cm^{-1}).[48] The NIR band can be decomposed in two main peaks, each accounting for about half the area of the band (λ_1 = 1066.2 nm, w_1 = 140.6 nm, 51.6%; λ_2 = 1025.1 nm, w_2 = 249.5 nm, 48.4% in $CHCl_3$; Figures S4 and S5). The NIR band displays a remarkable negative solvatochromism, with absorption maxima wavelengths ranging between 955 nm in DMF and 1060 nm in $CHCl_3$ (Table 1). On increasing the solvent polarity, the change in the experimental spectral shapes (Figure S6) suggests that the relative weight and the energy difference between the red-component and the main peak of the solvatochromic NIR band increases, so that a larger polar nature should be attributed to the higher energy peak as compared to the main one.

Theoretical Calculations. During the past decades, DFT calculations have been used successfully to investigate the structural features and the redox and spectroscopic properties of homoleptic and heteroleptic complexes containing 1,2-dithiolene ligands.[36–39,48,50,52,62,64,72] DFT calculations were applied here on Me$_2$timdt^{q-}, mnt^{q-} (q = 0, 1, 2) and related compounds, and the relevant neutral, monoanionic, and dianionic homoleptic and heteroleptic Pd complexes.

Ligands. The relative stability of the variously charged forms of 1,2-dithiolene ligands (Scheme 1) depends on the nature of the R substituents. The mnt ligand is generally encountered in its 1,2-dithiolate form, and the corresponding neutral species is unreported. In fact, neutral 1,2-dithiolene species are generally unstable,[6] but depending on the R substituents they can be found as either 1,2-dithiones (Scheme 1, b), for instance embedded in 1,2-**dithioxamides**,[119] or stabilized as 1,2-dithietes (Scheme 1, a).[120,121,122] Since vicinal dithioxamides in five-membered rings are reportedly unstable,[123] R'$_2$timdt ligands cannot be isolated as neutral 2,4,5-trithiones and the sulfuration of disubstituted 2-thioxomidazolidine-4,5-diones leads to tetrasubstituted 4,5,6,7-tetrathiocino[1,2-*b*:3,4-*b*']diimidazolyl-2,9-dithione or 4,5,9,10-tetrathiocino-[1,2-*b*:5,6-*b*']-2,7-dithione (a and b in Chart S4 in SI, respectively), the latter type of compounds being the final product of the Br_2 oxidation of [Pd(R'$_2$timdt)$_2$] complexes (R' = Et).[124] The only example of an authentic radical monoanion R"$_2$timdt$^{\bullet-}$ has been isolated in compound **5**.[72] Neutral 1,2-dithiolene ligands stabilized in the form of 3,4-disubstituted 1,2-dithietes have been characterized in few cases (R = CF_3,[120] $COOCH_3$,[121] 1-adamantyl[122]). An examination of the ZPE-corrected total electronic energies $\mathcal{E}^0_{ZPE}$ of the neutral 1,2-dithiolene ligands in the dithione and dithiete forms (Table 2) shows that the dithiete form is more favored for the mnt ligand as compared to the Me$_2$timdt one ($\Delta\mathcal{E}^0_{ZPE}$= 16.28 and –42.58 kcal/mol, respectively). A comparison of the C–C bond distance calculated for Me$_2$timdt^{q-} (d_{C-C} = 1.500, 1.434, and 1.394 Å for q = 0, 1, and 2, respectively; Table 2) can be done with the corresponding bond distances determined structurally in [Pd(Et$_2$timdt)Br$_2$] [average d_{C-C} value 1.47(1) Å; q = 0; Chart S2], **5** [d_{C-C} = 1.417(4) Å, q = 1; Chart S2],[48] [**6**·2Br]$^{2+}$(Br$_2$)$_2$(Br$_2$)$_3$ [**6** = 4,5,9,10-tetrathiocino-[1,2-*b*:5,6-*b*']-1,3,6,8-tetraethyl-diimidazolyl-2,7-dithione; d_{C-C} = 1.37(2) Å, q = 2; Chart S2], and 1,3-dimethyl-4,5-bis(phenylsulfanyl)-1,3-dihydro-2H-imidazole-2-thione [**7**, d_{C-C} = 1.361(6) Å, q = 2; Chart S2].[74] As expected, on passing from dianions to the corresponding neutral species the C–C bond lengths increase and the C–S distances decrease. It is worth noting that mnt^{q-} and Me$_2$timdt^{q-} (q = 0, 1, 2) share closely related frontier MO compositions (Figures S7 and S8). For both ligands, the KS-HOMO–1 and KS-HOMO of neutral species **L** are nonbonding molecular orbitals (NBMOs) built up of the in-phase and out-of-phase combinations, respectively, of the sulfur 3p AOs lying on the ligand plane. The LUMO is a π-in-nature MO deriving from the combination of C 2p$_z$ and S 3p$_z$ AOs of the ene-1,2-

dithiolate system, bonding with respect to the C–C bond and antibonding with respect to the C–S bonds. The LUMO of neutral **L** ligands becomes the SOMO and the HOMO in monoanionic $\mathbf{L}^{\bullet-}$ and dianionic $\mathbf{L}^{2-}$ species, respectively (Figures S7 and S8). The absolute reduction potential[105,125,126] E_{Abs}^{298K} (eq 7) of the redox step $\mathbf{L}/\mathbf{L}^{\bullet-}$ increases on passing from Me_2timdt to mnt (2.245 and 3.014 V, respectively), indicating that the mnt ligand displays the largest tendency to reduction. The difference in the E_{Abs}^{298K} values for the $\mathbf{L}/\mathbf{L}^{\bullet-}$ and $\mathbf{L}'/\mathbf{L}'^{\bullet-}$ couples, which only depends on the choice of the substituents R at the ene-1,2-dithiolate, can be considered a useful parameter to evaluate the "push" and "pull" nature[48,54] of 1,2-dithiolene ligands in heteroleptic mixed-ligand metal complexes $[M(\mathbf{L})(\mathbf{L}')]$.

Table 1. Experimental NIR absorption maxima wavelength λ (nm), energy *E* (eV), and FWHM values *w* on a wavelength scale (nm) recorded for 3, compared with the corresponding values λ_{calc} and E_{calc} calculated at TD-DFT IEF-PCM level (CS GS). Calculated oscillator strengths *f*, extinction coefficients $\varepsilon_{calc}^{corr}$ ($M^{-1}cm^{-1}$), and HOMO–LUMO energy gaps ΔE_{H-L} (eV) in selected media

	λ	λ_{calc}	E	E_{calc}	w	f	$\varepsilon_{calc}^{corr}$	ΔE_{H-L}
$CHCl_3$	1060	876.0	1.167	1.416	180	0.385	10700	1.68
CH_2Cl_2	1020	863.8	1.216	1.436	151	0.368	11895	1.73
THF	1011	864.4	1.226	1.435	168	0.368	10675	1.71
CH_3CN	966	843.9	1.284	1.469	236	0.340	6630	1.77
DMF	955	851.8	1.298	1.456	217	0.356	7712	1.77

Diradical Character (DC) in Bis(1,2-dithiolene) complexes. The ground state (GS) of neutral bis(1,2-dithiolene) complexes is characterized by a significant degree of DC,[33–37] due to the very narrow HOMO–LUMO energy gap ΔE_{H-L} that renders the singlet and triplet GSs very close in energy. In a pure diradical the non-bonding molecular orbitals (NBMOs) ψ_a and ψ_b hosting the two electrons at the highest energy are degenerate, being localized on the two different ligands in bis(1,2-dithiolene) metal complexes,[127] and they have consequently a negligible overlap integral $S_{ab} = \langle \psi_a | \psi_b \rangle$. Under these conditions, the two possible spin states, i.e. singlet (2S+1 = 1) and triplet (2S + 1 = 3), are degenerate, their energy difference $\Delta\mathcal{E}_{ST} = \mathcal{E}_S - \mathcal{E}_T$ being related to the exchange interaction $J = ½(\mathcal{E}_S - \mathcal{E}_T) = ½\,\Delta\mathcal{E}_{ST}$.[91] When S_{ab} is not negligible and the two NBMOs are quasi-degenerate, the triplet configuration is the most stable ($\mathcal{E}_S > \mathcal{E}_T$) and *J* assumes positive values in the so-called diradicaloids or diradical-like compounds. Wirz proposed to discriminate between diradicals and diradicaloids depending on the singlet-triplet energy gaps ($\Delta\mathcal{E}_{ST} \leq 10$ and 100 kJ mol^{-1} for diradicals and diradicaloids, respectively).[128] When the energy difference between the two involved MOs is larger and a significant gap exists, the energy stabilization competes with the electron-electron exchange interaction, and the CS singlet GS becomes progressively more stable. The theoretical evaluation of the GS in diradical and diradicaloid species is a challenging task, which requires the evaluation of the stability of the triplet and singlet GSs of the investigated compound. Triplet GS can generally be calculated by theoretical methods with unrestricted wavefunctions, such an unrestricted HF (UHF) or Density Functional Theory (UDFT). The modeling of open-shell singlet diradicals requires multireference approaches, for instance multireference coupled-cluster calculations, such as Mk-CCSD(T),[129] complete active-space self-consistent field (CASSCF),[94] or the complete-active-space second-order perturbation theory (CASPT2).[130] In fact, although computationally very efficient, DFT calculations cannot describe accurately open-shell singlet states of diradicals, so that $\Delta\mathcal{E}_{ST}$ and hence *J* values are largely uncertain. The broken-symmetry (BS) DFT (DFT-BS) spin unrestricted reference configuration with antiparallel spins has been proposed as a compromise to extend UDFT calculations to diradical species,[91,131,132,133,134,135] by correcting *J* and $\Delta\mathcal{E}_{ST}$ for spin contamination[94,133,134] that affects the expectation value of the total spin $\langle S^2 \rangle$ with respect to $\langle S(S+1) \rangle$.[94,95,136] In different studies, the DC index n_{DC} of homoleptic bis(1,2-dithiolene) complexes was evaluated. A comparison of n_{DC} calculated at different levels of theory suggests that the DFT-BS approach underestimate the DC of bis(1,2-dithiolene) metal complexes. In fact, the DC of the neutral complex

Table 2. Optimized C–C and C–S bond distances (d_{C-C} and d_{C-S}, Å) within the 1,2-dithiolene moiety and corresponding Wiberg bond indices (WBI_{C-C} and WBI_{C-S}), variations in ZPE corrected total electronic energies ($\mathcal{E}_{ZPE}^0 = \mathcal{E}^0 + ZPE$, kcal mol^{-1}), sum of electronic energies $\mathcal{E}^0$ and thermal enthalpies (H_{corr}, kcal mol^{-1}) and free energies (G_{corr}, kcal mol^{-1}) calculated for the 1,2-dithiolene ligands mnt^{q-} and Me_2timdt^{q-} (q = 0, 1, 2)

	q	d_{C-C}	d_{C-S}	WBI_{C-C}	WBI_{C-S}	$\Delta\mathcal{E}_{ZPE}^0$	$\Delta(\mathcal{E}^0 + H_{corr})^c$	$\Delta(\mathcal{E}^0 + G_{corr})^d$
mnt^a	0	1.501	1.625	1.018	1.787	–	–	–
mnt^b		1.371	1.756	1.501	1.100	-16.28[e]	-16.58[e]	-15.46[e]
Me_2timdt^a		1.500	1.629	1.007	1.712	–	–	–
Me_2timdt^b		1.343	1.765	1.538	1.061	42.58[e]	41.28[e]	45.27[e]
mnt^-	1	1.431	1.681	1.397	1.235	-84.47[f]	-84.58[f]	-84.09[f]
Me_2timdt^-		1.434	1.675	1.217	1.423	-51.33[f]	-51.35[f]	-50.90[f]
mnt^{2-}	2	1.406	1.736	1.365	1.178	-34.75[f]	-34.87[f]	-33.87[f]
Me_2timdt^{2-}		1.394	1.738	1.453	1.201	13.09[f]	13.07[f]	14.23[f]

[a] 1,2-Dithione form. [b] 1,2-Dithiete form. [c] Sum of electronic and thermal enthalpies. [d] Sum of electronic and thermal free energies. [e] Relative energy difference between the 1,2-dithiete and the 1,2-dithione form: $\Delta\mathcal{E}^0 = \mathcal{E}^0(\text{dithiete}) - \mathcal{E}^0(\text{dithione})$. [f] Relative energy difference between reduced and neutral species: $\Delta\mathcal{E}^0 = \mathcal{E}^0(\text{reduced}) - \mathcal{E}^0(\text{neutral})$.

$[Ni(bdt)_2]$ (bdt^{2-} = benzene-1,2-dithiolate) was calculated to be as large as 69.1% at CASSCF level,[37] 32% at ZORA-SORCI level (ZORA = zeroth-order regular approximation; SORCI = spectroscopy oriented configuration interaction),[33] and 17.2% at DFT-BS level. The DC depends not only on the 1,2-dithiolene ligand, but also on the nature of the central metal ion. In the series of complexes of M^{II} ions deriving from the 3,5-di-tert-butyl-1,2-benzenedithiolato ligand, the n_{DC} was calculated in 32%, 50%, and 30% for M = Ni, Pd, and Pt, respectively,[33] suggesting that Pd^{II} species may show singlet diradicals particularly stable as compared to the corresponding Ni^{II}/Pt^{II} analogues.

Homoleptic Bis(1,2-dithiolene) complexes. Members of the class of complexes $[M(R'_2timdt)_2]^{q-}$ (M = Ni, Pd, Pt; q = 0, 1, 2) are mostly stable as neutral species, and quite severe conditions are needed to achieve the reversible chemical or electrochemical reduction to the corresponding monoanionic radical species.[16,46,48,52] As regards M = Pd, while the crystal structures of $[Pd(Et_2timdt)_2]$ and the CT adduct $[Pd(Et_2timdt)_2]\cdot I_2\cdot CHCl_3$ have been long since published,[45] no anionic complexes $[Pd(R'_2timdt)_2]^{-/2-}$ have been structurally characterized so far. Conversely, $[M(mnt)_2]$ neutral complexes (M = Ni, Pd, Pt) are extremely rare, and $(perylene)_2$(**4**) is the only compound characterized structurally incorporating the neutral species **4**,[116] while to date 37 examples of compounds incorporating the anions $\mathbf{4}^{-/2-}$ have been deposited to the Cambridge Crystallographic Database.[137] Accordingly, **1** is calculated to be sensibly more stable to reduction in the gas phase and in CH_2Cl_2 than **4** (E_{Abs}^{298K} = 3.057 and 4.349 eV for complex **1**; 4.786 and 5.752 eV for complex **4**, in the gas phase and in CH_2Cl_2, respectively). In Table 3, the metric parameters optimized for the bis(1,2-dithiolene) complexes $\mathbf{1}^{q-}$ and $\mathbf{4}^{q-}$ (q = 0, 1, 2) are summarized. In the case of neutral complexes (q = 0), the geometry was optimized (i) for the singlet CS (RDFT), (ii) for the triplet open-shell (UDFT), and (iii) for the singlet diradical (DFT-BS) GS configurations. The total electronic energy $\mathcal{E}_T$ of the $^3B_{1u}$ triplet state is calculated to be lower by about 2.4 kcal mol^{-1} (10 kJ mol^{-1}) as compared to that ($\mathcal{E}_S$) of the uncorrected singlet ^1A_g GS ($\mathcal{E}_2 < 0$, eq 2), thus classifying **1** as a diradical species.[128] In fact, the DFT-BS GS of **1** shows a large $< S^2 >_{BS}$ value (0.80, Table 4), indicating a considerable spin contamination from the triplet state.[94] An evaluation of the total electronic energy of the BS GS shows that it is the most stable configuration as compared both to the triplet and CS-singlet configurations (eq 1), reflected in a diradical character n_{DC} = 55.4% (Table 4, eq 5). The singlet GS calculated for **4** is sensibly lower in energy as compared to the relevant triplet state (Table 4), indicating a diradicaloid character. Accordingly, the singlet diradical configuration is only slightly more stable than the uncorrected CS singlet state and shows $< S^2 >_{BS}$ smaller than 0.5. In fact, the spin-contamination corrected state (eq 4) was found to be the most stable one with only a partial diradical character (n_{DC} = 27.5%, Table 4). A comparison between structural and DFT-optimized bond distances for complexes **1** and **4** shows that Pd–S and C–C distances are slightly overestimated, while C–S bond lengths are very close. Pd–S bond lengths are very sensitive to the GS configuration and follow the trend Pd–S (triplet) > Pd–S (CS singlet) ≥ Pd–S (singlet diradical) > Pd–S (structure). The C–S bond distances optimized for the singlet diradical GSs of **1** and **4** (1.699 Å; Table 3) are very close to those calculated for the hypothetical free $Me_2timdt^{\bullet-}$ and $mnt^{\bullet-}$ radical anions (1.681 and 1.675 Å, respectively), but sensibly different from those calculated for the relevant 1,2-dithiones and 1,2-dithiolates (Table 2). This supports the description of neutral homoleptic complexes as $[Pd(\mathbf{L}^{\bullet-})_2]$ for both classes of complexes. Although the agreement between structural and optimized C–C distances is less accurate as compared to C–S bond lengths, the former values are affected very largely by the charge on the ligands.

Table 3. Optimized Pd–S, C–C, and C–S bond lengths (d, Å), and Wiberg bond indices (WBI) within the 1,2-dithiolene ligands L and L' of $[Pd(L)(L')]_2^{q-}$ complexes (L = L' = Me_2timdt for $\mathbf{1}^{q-}$; L = Me_2timdt, L' = mnt for $\mathbf{3}^{q-}$; L = L' = mnt for $\mathbf{4}^{q-}$; q = 0, 1, 2). For neutral species (q = 0), the distances in the open-shell paramagnetic triplet, CS diamagnetic singlet, and singlet diradical (BS) configurations are reported

	GS	Symm.[a]	L					L'					
			d_{Pd-S}	d_{C-C}	d_{C-S}	WBI_{C-C}	WBI_{C-S}	d_{Pd-S}	d_{C-C}	d_{C-S}	Δd_{C-C}[b]	WBI_{C-C}	WBI_{C-S}
1	Triplet	$^3B_{1u}$	2.351	1.410	1.698	1.177	1.378						
	Singlet	^1A_g	2.314	1.404	1.697	1.269	1.276						
	BS	–	2.307	1.401	1.699	1.251	1.274						
Struct. $[Pd(Et_2timdt)_2]$[c,d]			2.295(2)	1.397(9)	1.689(8)								
$\mathbf{1}^-$	Doublet	$^2B_{2g}$	2.337	1.381	1.717	1.385	1.192						
$\mathbf{1}^{2-}$	Singlet	^1A_g	2.376	1.365	1.739	1.482	1.126						
3	Triplet	$^3B_1$	2.359	1.408	1.700	1.226	1.267	2.305	1.404	1.701	0.004	1.307	1.098
	Singlet	$^1B_1$	2.342	1.428	1.674	1.168	1.397	2.263	1.393	1.725	0.035	1.417	1.098
	BS	–	2.344	1.422	1.682	1.186	1.354	2.273	1.389	1.717	0.033	1.384	1.098
Struct. **3**[e]			2.314(2)	1.454(16)	1.660(8)			2.258(2)	1.364(16)	1.724(8)	0.090		
$\mathbf{3}^-$	Doublet	$^2A_1$	2.369	1.397	1.697	1.290	1.276	2.286	1.376	1.740	0.021	1.451	1.138
$\mathbf{3}^{2-}$	Singlet	$^1B_1$	2.384	1.364	1.737	1.477	1.131	2.323	1.381	1.744	-0.017	1.424	1.130
4	Triplet	$^3B_{1u}$	2.325	1.410	1.696	1.277	1.329						
	Singlet	^1A_g	2.275	1.403	1.701	1.325	1.305						
	BS	–	2.289	1.451	1.699	1.311	1.312						
$\mathbf{4}^-$	Doublet	$^2B_{2g}$	2.295	1.386	1.725	1.405	1.195						
$\mathbf{4}^{2-}$	Singlet	^1A_g	2.332	1.380	1.743	1.428	1.131						
Struct. **4**[d,f]			2.263(7)	1.39(2)	1.71(1)								

[a] GS-symmetry representations are referred to the D_{2h} (**1**, **4**) and C_{2v} (**3**) point groups, with the complex molecule laying on the *yz* plane, and the main axis being coincident with *z*. [b] Δd_{C-C} = difference in d_{C-C} values calculated within the two ligands $Me_2timdt^{-q/2-1}$ and $mnt^{-q/2-1}$ in $\mathbf{3}^{q-}$. [c] Ref. 45. [d] Average value. [e] This work. [f] Isolated in $(perylene)_2$(**4**), ref. 116.

In Figure 3, the optimized C–C distances and the corresponding Wiberg bond indices (WBIs)[97] are compared for a variety of R_2timdt derivatives showing a C–C double bond, such as the 4,5,9,10-tetrathiocino[1,2-*b*:5,6-*b*']diimidazolyl-1,3,6,8-tetramethyl-2,7-dithione $(Me_2timdt)_2$ and the compound **7**,[74] or a single bond as in the neutral complex **2** and in compound **5** (Chart S2).[72,73] For these compounds, a clear correlation (R^2 = 0.999) holds between the optimized C–C bond distance d_{C-C} within the R_2timdt ring and the corresponding WBI_{C-C} values. This clearly shows that WBIs calculated at the optimized distances represent a reliable parameter in evaluating the charge distribution and hence the oxidation state of non-innocent 1,2-dithiolene ligands. When 1,2-dithiolene complexes $\mathbf{1}^{q-}$ (q = 0, 1, 2) are considered, the d_{C-C} and WBI_{C-C} data, while not exactly fitting the correlation, point out that complex $\mathbf{1}^{2-}$ falls in the area of C=C double bonds, very close to $(Me_2timdt)_2$ and compound **7**, therefore confirming the 2-thioxoimidazoline-4,5-dithiolate nature of the ligands in the dianionic complex.

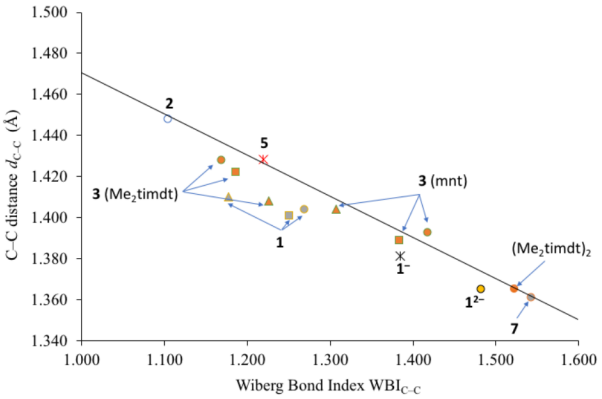

Figure 3. Correlation between optimized C–C bond distances (d_{C-C}) and Wiberg bond indices (WBI_{C-C}) within the 1,2-dithiolene ligand calculated for selected systems (circle = singlet; star = doublet; triangle = triplet; square = singlet diradical).

Complexes **1** (whatever the approach adopted for describing its GS) and $\mathbf{1}^-$ fall in the central area of the graph, indicating an intermediate character of the C–C bond between a single and a double bond. An examination of the frontier KS-MOs composition shows that according to the CS description of the GS of **1**, the KS-HOMO and the KS-LUMO are π–MOs represented by the b_{3u} in-phase and b_{2g} out-of-phase combinations of the singly occupied molecular orbitals (SOMOs) of the two $Me_2timdt^{\bullet-}$ ligands (Figure 4a; Figure S8). In fact, the b_{3u} KS-HOMO (MO 107 according to a progressive labeling based on an energy scale) is mainly made up of the four $3p_x$ AOs of the four donor S-atoms, perpendicular to the molecular *yz* plane and the four C $2p_x$ AOs taken with opposite phases. The terminal S-atoms also participate to this MO, while the contribution from the central Pd ion is very poor (4%). The 108 b_{2g} KS-LUMO involves the same atomic species as the HOMO with a larger contribution from the bonding sulfur atoms, but the contributions from the two ligands are opposite in phase. In the KS-LUMO, the metal ion is as well only marginally involved (5%) through its $3d_{yz}$ AOs. In the singlet diradical DFT-BS GS configuration, the α and β-HOMOs show the same composition as the HOMOs of the constituent 1,2-dithiolene $Me_2timdt^{\bullet-}$ ligands, analogously to what was previously reported for different Ni and Pt bis(1,2-dithiolene) metal complexes,[52] the central Pd ion participating to both α and β MOs (3%). Notably, the DFT-BS approach results in a stabilization of the KS-HOMO and destabilization of the KS-LUMO with respect to the restricted CS solution, thus increasing ΔE_{H-L} gap (Figure 5, top). The CS description of complex **1** features a single allowed NIR one-electron excitation calculated at TD-DFT level. This corresponds to the $^1A_g \rightarrow {}^1B_{1u}$ transition, involving almost exclusively (97%) the one-electron HOMO-LUMO (H→L) excitation. This is calculated to fall at 963.0 nm (oscillator strength f = 0.436) in the gas phase and 1068.3 nm (f = 0.581) in CH_2Cl_2. The oscillator strength calculated at TD-DFT level along with experimental FWHM value of the NIR band were used to evaluate a molar extinction coefficient ε for **1** (eq 6).[101] The symmetric and antisymmetric combinations of the α–107→α–108 and β–107→β–108 excitation (H,H→L,L double exciton states) are calculated as BS-GS→ES 1 and BS-GS→ES 2 transitions. Double exciton states have been reported for conjugated chromophores with open-shell diradical character,[127] such as polyenes[138,139] and quinoidal oligothiophenes.[140] The double exciton state is one-photon forbidden and it has been observed as a weak band at lower energies than the main absorption band due to the one-photon allowed single exciton state.[127] The symmetry-allowed transition BS-GS→ES 2 falls at wavelength values sensibly lower (E = 1.487 eV, λ_{max} = 833.6 nm, f = 0.310) than that predicted for the singlet GS (see above). The complex envelope of the NIR absorption band of [M(R,R'timdt)$_2$] neutral bis(1,2-dithiolene) complexes can be attributed to the contribution of doubly excited states to the main single exciton states, thus possibly accounting for the unusually high molar extinction coefficients observed to the NIR absorption in this class of bis(1,2-dithiolene) complexes.[46,49] The forbidden BS-GS→ES 1 transition (1.142 eV, λ_{max} = 1085.6 nm) may provide a low-energy weak contribution[138] to the NIR absorption due to the vibronic coupling with the B_{1u} antisymmetric combination of the stretching Pd–S vibrations, calculated at 294.1 and 293.2 cm^{-1} at RDFT and DFT-BS level, respectively.

Table 4. Singlet broken–symmetry (ε_1), singlet–triplet (ε_2) energy differences, spin contamination corrected singlet-triplet energy gap ($\Delta\varepsilon_{ST}^{SC}$; kcal mol^{-1}), expectation value of the spin contaminant $\langle S^2\rangle_{BS}$ for the singlet diradical configuration, effective electron exchange integrals J_{ab} and diradical character n_{DC}(%) calculated for complexes 1, 3, and 4.

	1	**3**	**4**
ε_1	-4.325	-0.789	-1.015
ε_2	-2.404	5.817	6.197
$\Delta\varepsilon_{ST}^{SC}$	3.986	-7.420	-8.096
$\langle S^2\rangle_{BS}$	0.801	0.436	0.474
$\lvert J_{ab}\rvert$	1.579	4.175	4.664
n_{DC}(%)	55.4	24.9	27.5

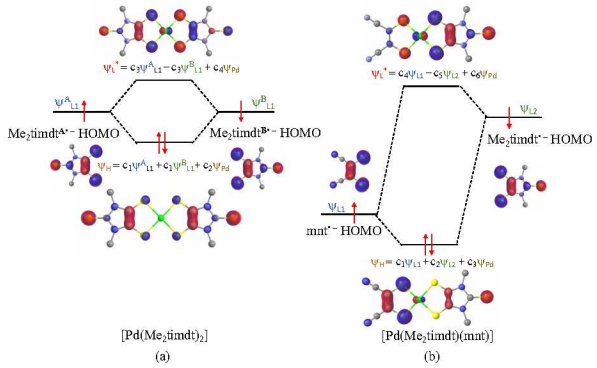

Figure 4. Qualitative MO diagram showing the contributions of the HOMOs of the 1,2-dithiolene ligands to the HOMO and LUMO of complex **1** (a; c_1 = 48%, c_2 = 4%; c_3 = 47.5%, c_4 = 5%) and complex **3** (b; c_1 = 61%, c_2 = 31%, c_3 = 8%; c_4 = 24%, c_5 = 70%, c_6 = 6%) in the CS GS description. In the KS-MO drawings hydrogens have been omitted for clarity. Cutoff value = 0.05 |e|.

Electronic structure of [Pd(Me₂timdt)(mnt)] (3). The GS geometry for **3** (E_{Abs}^{298K} = 3.784 and 4.872 eV in the gas phase and CH_2Cl_2, respectively) was optimized in its singlet CS ($^1B_1$), triplet open shell ($^3B_1$) and singlet diradical (BS) configurations. The triplet-singlet energy gap classifies **3** as a diradicaloid (Table 4).[91,128] While the $^3B_1$ state is sensibly less stable than the singlet state, the singlet diradical BS ($< S^2 >_{BS}$ = 0.436) and the $^1B_1$ CS singlet configurations differ by less than 1 kcal mol^{-1} (Table 4). The singlet configurations calculated at RDFT and DFT-BS level show very close optimized Pd–S, C–C, and C–S bond distances, only very slightly overestimated (by less than 0.03 Å) as compared to the relevant structural ones (Table 3). The difference $\Delta d_{C\text{-}C}$ between the C–C bond distances $d_{C\text{-}C}$ of the two 1,2-dithiolene ligands [corresponding to the C(1)–C(1)^i and C(4)–C(4)^i structural bond lengths in Figure 1 for the Me₂timdt and mnt ligands, respectively] is evaluated correctly [C(1)–C(1)^i > C(4)–C(4)^i], but it is slightly underestimated, so that the calculated dithione-dithiolato character is less pronounced than expected based on the structural data (Table 3). The DFT-BS description of the GS provides a lowest $\Delta d_{C\text{-}C}$ value than the CS description. Accordingly, while the charge Q_{Pd} on the central Pd ion in the CS and in the singlet diradical GSs is essentially unchanged (ΔQ_{Pd} = 0.024 |e|), the difference in the charges calculated on the two 1,2-dithiolene ligands at NBO level is sensibly larger in the former (0.514 and 0.390 |e|, respectively). In the RDFT approach, the optimized values for the C–C distances of the Me₂timdt and mnt ligands correspond to noticeably different WBIs (1.168 and 1.417 in the $^1B_1$ CS GS), and clearly fall in different regions of the $d_{C\text{-}C}$ vs $WBI_{C\text{-}C}$ correlation (Figure 3).Therefore, the comparison between structural and DFT-optimized data indicates that the CS description is sensibly more suitable than the singlet diradical one in modeling the GS of the mixed-ligand complex **3**. Notably, the values of the C–C bond lengths within the mnt ligand in **3** (1.393 Å, Table 3) is even shorter than the value calculated for the free mnt^{2-} ligand (1.406 Å, Table 2). On passing from **3** to the radical anion **3**$^-$ and the dianion **3**$^{2-}$, only minor differences (lower than 0.02 Å) are observed on the mnt ligand, while the Me₂timdt is more largely affected, the $d_{C\text{-}C}$ distance being progressively shortened ($d_{C\text{-}C}$ = 1.428, 1.397, and 1.364 Å within the Me₂timdt ligand for **3**, **3**$^-$, and **3**$^{2-}$, respectively; Table 3). In summary, the comparison between calculated and experimental data supports the hypothesis that the GS of **3** can be better described as a dithione-dithiolato [Pd^{II}(Me₂timdt)(mnt^{2-})] complex with a minor contribution from the singlet diradical [Pd^{II}(Me₂timdt$^{\bullet-}$)(mnt$^{\bullet-}$)] description. Accordingly, a diradical character n_{DC} = 24.9% (eq 5) is calculated for complex **3** (Table 4).[141] The KS-HOMO and KS-LUMO in the CS description (MO 93 and 94, respectively) are π-in-nature MOs mainly located on the mnt (61%) and Me₂timdt (70%) ligands, respectively, with only minor contributions from the 4d_{xz} AO of the Pd central atom (6% and 8%, respectively; Table S7). Hence, KS-HOMO and KS-LUMO in the heteroleptic complex can be considered as deriving from the in-phase and out-of-phase combinations of the SOMOs of the constituent ligands mnt$^{\bullet-}$ and Me₂timdt$^{\bullet-}$ (Figure 4b; Figures S7 and S8). The former ("pull" electron-withdrawing ligand, HOMO at lower energy) contributes mostly to the KS-HOMO of **3** and assumes a larger character of 1,2-dithiolate, while the latter ("push" ligand, HOMO at higher energy) contributes mostly to the KS-LUMO of **3** and assumes a larger character of 1,2-dithione, in agreement with the structural data discussed above. In the DFT-BS description, the eigenvalues of the corresponding α and β MOs are sensibly unequal, reflecting their different compositions [Figure 5 (bottom) and Figure S9]. In particular, the α-MO 93 is located on the mnt ligand [76%; Table S8 and (a) in Figure S9], while the β-MO 93, less stable, largely on the Me₂timdt ligand [63%; Table S8 and (c) in Figure S9]. Conversely, the α-MO 94 is located almost entirely on the Me₂timdt ligand [91%; Table S8 and (b) in Figure S9], while the β-MO 94 shows contributions from both ligands [mnt 54%, Me₂timdt 36%; Table S8 and (d) in Figure S9].

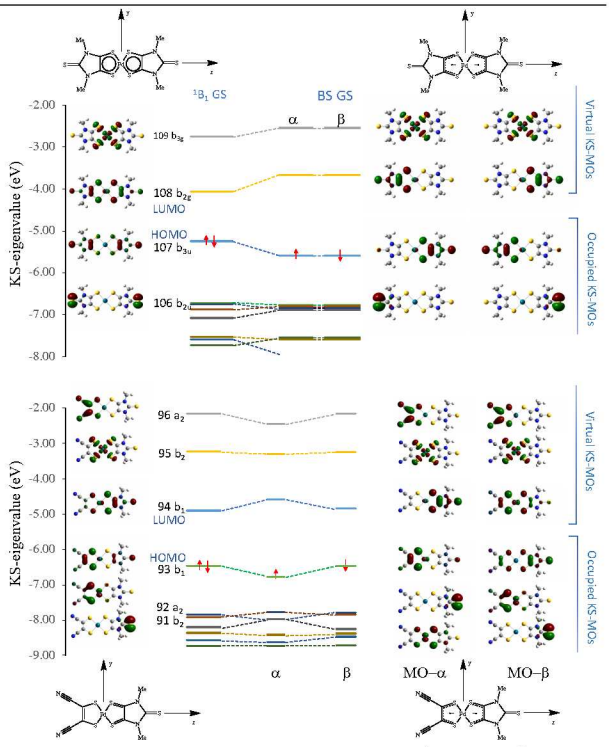

Figure 5. Frontier KS-MOs energy diagram (-2 – -8 eV) showing the energy and MO drawing in the restricted (CS GS, left) and singlet diradical (BS GS, right) descriptions for **1** (top) and **3** (bottom). Cutoff value = 0.05 |e|.

Therefore, both the RDFT and DFT-BS approaches agree in attributing a LL'CT character to the lowest energy transition, from the mnt "pull" ligand to the Me_2timdt "push" ligand. TD-RDFT calculations show, in excellent agreement with experimental data (Figure 2 and Figure S3 in SI), three main spectral regions, namely (i) an overlap of intense transitions in the UV region ($\lambda < 280$ nm), (ii) a band in the visible region ($300 \leq \lambda \leq 500$ nm), and (iii) the single very intense NIR transition ($\lambda > 800$ nm). In Figure 6, the UV–vis–NIR spectrum of **3** in $CHCl_3$ solution, simulated based on singlet IEF-PCM TD-RDFT calculations (Table 5), is depicted. The absorption bands in the UV region are due to the overlap of several peaks involving the frontier orbitals, with intraligand (GS→ES 9), interligand (GS→ES 13), or ligand-to-metal (GS→ES 15 and GS→ES 17) character. The absorption in the visible region is mainly due to the GS→ES 7 intraligand transition, involving mainly the KS-HOMO–3 and KS-LUMO, centered on the Me_2timdt ligand and the Pd^{II} ion. A single intense transition is calculated in the NIR region, falling at 1.489 eV (Table 4). This transition involves almost exclusively (88.4%) the one-electron excitation from the KS-HOMO (MO 93) to the KS-LUMO (MO 94). Notably, the oscillator strength f calculated for the NIR transition (0.315) is sensibly lower than that calculated for **1** ($f = 0.436$, see above), in agreement with the experimental values determined for the corresponding molar extinction coefficients. TD-RDFT calculations were carried out at the IEF-PCM level of theory in the same solvent systems experimentally adopted to record UV–vis–NIR spectra. The calculated NIR transition energies are generally overestimated but linearly correlated to the experimental ones [$R^2 = 0.88$; E_{calc} (eV) = 0.374 E_{exp} + 0.979; Table 1 and Figure S10]. Both in the gas phase and in the solvents considered at IEF-PCM level, the NIR transition is attributed exclusively to the H→L one-electron excitation. Accordingly, a linear correlation holds between the calculated transition energies in the NIR region and the ΔE_{H-L} energy gap evaluated in each of the examined solvents (Table 1; $R^2 = 0.92$). Along the series $CHCl_3$, CH_2Cl_2, THF, CH_3CN, DMF the contribution of the mnt fragment to KS-HOMO and KS-LUMO slightly increases (68% to 70%) and decreases (16% to 13%), respectively (Table S7).

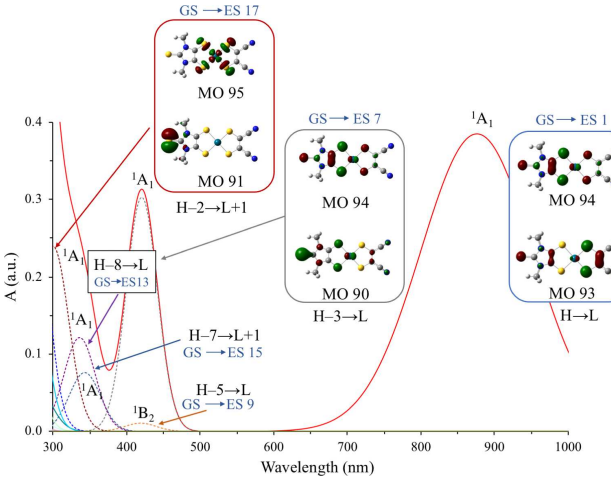

Figure 6. UV–vis–NIR spectrum of **3** simulated based on IEF-PCM TD-RDFT calculations in $CHCl_3$. FWHM $w = 90$ nm for the $^1A_1$ (H→L) transition, $w = 25$ nm for the UV–vis bands. Cutoff value = 0.05 |e|.

The contribution of the Me_2timdt fragment to KS-HOMO and to KS-LUMO decreases (23% to 20%) and increases (78% to 82%), respectively. Therefore, on passing to $CHCl_3$ to DMF, the NIR transition assumes a larger LL'CT character, and the ΔE_{H-L} energy gap increases from 1.68 eV in $CHCl_3$ to 1.77 eV in DMF and CH_3CN, in agreement with the experimental trend of NIR absorption energies (Table 1). Calculated oscillator strengths f fall between 0.356 and 0.385 in DMF and $CHCl_3$, respectively (Table S9). Oscillator strength values calculated at TD-DFT level have been used along with experimental full widths at half-maximum (FWHM, w) to evaluate the ratio between the extinction coefficient in each solvent and that in $CHCl_3$ solution. The resulting scaled calculated extinction coefficients $\varepsilon_{calc}^{corr}$ (Table 1) progressively decrease on increasing the transition energies. TD-DFT calculations were carried out on **3** in the singlet diradical electron configuration. Since the two α-93→α-94 and β-93→β-94 (H→L) excitations are not degenerate (Figure 5, bottom), the α-excitation contributes mainly (58.1%) to the symmetry-allowed transition at higher energy [0.853(α-93→α-94)–0.464(β-93→β-94); E = 1.629 eV, λ = 761 nm, $f = 0.267$ in the gas phase], while the β-excitation to the one at lower energy [0.486(α-93→α-94)+0.881(β-93→β-94); E = 0.746 eV, λ = 1663 nm, $f = 0.033$], forbidden in the C_{2v} point group. Although the contribution of the singlet diradical description to the GS of **3** is limited, it is conceivable that the former transition, corresponding to a double exciton state, can provide a high-energy component to the NIR transition. Notably, due to its nature, the double exciton transition is predicted to show remarkable solvatochromic effects, thus accounting for the different spectral shapes observed on varying the solvent (Table 1 and Figure S6).

Finally, the lack of inversion center in the title complexes suggests a possible application of heteroleptic bis(1,2-dithiolene) complexes as second-order nonlinear optical (SONLO) materials. Prompted by the results obtained at TD-DFT level, since small geometrical differences can determine large differences on NLO properties,[38,39] static dipole moments (μ) and static first (quadratic) hyperpolarizabilities (β_{tot}) were calculated for **3** in the gas phase, in CH_2Cl_2, and in $CHCl_3$ solutions (Table S10).[109] Calculations were also carried out at DFT-BS level (Table S10) in the gas phase. For the sake of comparison, the same calculations were also undertaken, at the same level of theory, on [Pt(phen)(tdt)] (phen = 1,10-phenanthroline; tdt^{2-} = 3,4-toluenedithiolate; Chart S2), a neutral diimine-dithiolate Pt complex showing a very large hyperpolarizability value among those investigated experimentally by means of EFISH measurements ($\lambda_{max} = 583$ nm; $\beta_\mu = -28 \cdot 10^{-30}$ esu with $\omega = 1.569 \cdot 10^{11}$ GHz; zero-frequency $\beta_0 = -16 \cdot 10^{-30}$ esu).[71] In agreement with the charge distribution within complex **3**, the μ vector lies along the molecular z axis and β shows only tensor z-components. As previously observed for different heteroleptic metal complexes containing 1,2-dithiolato ligands,[62] a dramatic increase in β_{tot} was calculated when solvation is taken into account ($|\beta_{tot}| = 37.6 \cdot 10^{-30}$, $475.6 \cdot 10^{-30}$, and $330.5 \cdot 10^{-30}$ esu in the gas phase, CH_2Cl_2, and $CHCl_3$, respectively). In addition, when the diradical character of **3** is evaluated at DFT-BS level, the β_{tot} value dramatically increases ($177.4 \cdot 10^{-30}$ esu in the gas phase), reaching the same order of magnitude computed for [Pt(phen)(tdt)].

Table 5. Energy *E* (eV), wavelength λ (nm), and oscillator strength *f* of main ($f \geq 0.005$) UV–vis–NIR electronic transition calculated for 3 in the gas phase, in CH_2Cl_2, and $CHCl_3$ at IEF-PCM TD-RDFT level[a]

		Gas phase			$CHCl_3$			CH_2Cl_2			
ES[b]		*E*	λ	*f*	*E*	λ	*f*	*E*	λ	*f*	Main contributions
1	$^1A_1$	1.489	832.6	0.315	1.415	876.0	0.385	1.436	863.8	0.368	H (93)→L (94, 100%)
7	$^1A_1$	2.931	423.0	0.153	2.950	420.3	0.303	2.974	416.9	0.324	H-3 (90)→L (94, 91%)
9	$^1B_2$	2.983	415.7	0.009	2.962	418.6	0.011	2.966	418.0	0.008	H-5(88) →L (94, 92%)
13	$^1A_1$	3.586	345.8	0.096	3.691	335.9	0.121	3.719	333.4	0.122	H-8 (85)→L (94, 91%)
15	$^1B_2$	3.787	327.4	0.046	3.616	342.9	0.076	3.583	346.1	0.076	H-7(86)→L+1(95,15%), H(93)→L+2(96, 75%)
17	$^1A_1$	4.133	300.1	0.121	4.135	299.9	0.240	4.132	300.1	0.250	H-2 (91)→L+1 (95, 96%)
20	$^1B_2$	4.364	284.2	0.005	4.294	288.8	0.007	4.274	290.1	0.006	H-13(80)→L+1 (95, 19%), H-9 (84)→L+1 (95, 65%)

[a] KS-HOMO (H) = MO 93; KS-LUMO (L) = MO 94. [b] Excited state (ES) numbering taken from gas-phase calculations.

CONCLUSIONS

DFT calculations have been exploited to investigate the structural and spectroscopic features of the heteroleptic mixed-ligand Pd^{II} bis(1,2-dithiolene) neutral complex **3**, to highlight the differences with the homoleptic related complexes **1** and **4**, and to develop sound structure-property relationships. The closed-shell (CS) description is only partially suitable to describe the electronic structure of bis(1,2-dithiolene) complexes, and – whatever the nature of the ligands – the singlet diradical character (DC) must be taken into account. The broken-symmetry (BS) approach within DFT, although itself a dramatic approximation underestimating the DC of bis(1,2-dithiolene) metal complexes, is a useful tool in supplementing the description of the ground state (GS). Few general conclusions can be drawn:

1) The nature of the 1,2-dithiolene ligand is responsible for the relevance of diradical character (DC) in the GS of 1,2-dithiolene complexes. In homoleptic neutral bis(1,2-dithiolene) complexes, on passing from complex **4** to complex **1**, the n_{DC} index is roughly doubled. This can be related to the capability of the ligands $mnt^{\bullet-}$ and $Me_2timdt^{\bullet-}$, respectively, to stabilize the unpaired electron. In heteroleptic mixed-ligand complexes, the absolute one-electron reduction potentials E_{Abs}^{298K} calculated for the $\mathbf{L}/\mathbf{L}^{\bullet-}$ and $\mathbf{L'}/\mathbf{L'}^{\bullet-}$ couples can be used to evaluate the nature of the $[Pd^{II}(\mathbf{L})(\mathbf{L'})]$ complex. The 1,2-dithiolene ligand displaying the largest reduction potential ("pull" ligand) features its π-NBMO at lower energy and contributes largely to the KS-HOMO of the heteroleptic complex, while that with the lowest potential ("pull" ligand) to the KS-LUMO. As a consequence, it is conceivable that the difference ΔE_{Abs}^{298K} in the absolute reduction potentials of the ligands **L** and **L'** can be adopted as a useful parameter to estimate the push-pull nature of the resulting heteroleptic neutral complexes $[Pd^{II}(\mathbf{L})(\mathbf{L'})]$ and the different localization of KS-HOMO and KS-LUMO. A larger push-pull character points to a larger dithione-dithiolato nature and a lower DC of the complex. This implies that the DC is the largest in homoleptic bis(1,2-dithiolene) complexes $[Pd^{II}(\mathbf{L})_2]$ with ligands **L** featuring low values of E_{Abs}^{298K}, such as Me_2timdt, and decreases in heteroleptic complexes $[Pd^{II}(\mathbf{L})(\mathbf{L'})]$ in dependence on ΔE_{Abs}^{298K}.

2) Several authors have observed that metal-sulfur bond lengths optimized at DFT level are slightly overestimated as compared to structural bond distances. This can be attributed to the use of RDFT calculations in complexes featuring a significative DC. The DFT-BS approach leads to bond distances closer to the structural ones. It can be deduced that in the case of complexes with a large DC, such as complex **1**, the difference between CS-optimized distances and the relevant experimental metric parameters increases with the DC of the complex.

3) The spectral shape of the NIR band of neutral bis(1,2-dithiolene) metal complexes has been indicated to be a complex envelope resulting from a series of *d*–*d* transitions with different spin coupling to the open-shell ligands. The intensity of this band, peculiar to metal bis(1,2-dithiolene) complexes, may be attributed not only to the very large oscillator strength *f* calculated for the HOMO-LUMO one-electron excitation within a CS description, but also to the contribution of double exciton states typical of diradical species. To a lower extent, double exciton states are possible also in heteroleptic bis(1,2-dithiolene) complexes and can be related with the spectral shapes observed for the NIR band in different solvents.

4) The intrinsic optical nonlinearity of heteroleptic bis(1,2-dithiolene) complexes is enhanced by their DC, providing a further criterion, in addition to the lack of inversion center and large electric dipole values, for the rational design of NLO materials active in the vis-NIR region.

Summarily, this investigation shows that the DC of bis(1,2-dithiolene) metal complexes can be extensively modulated by means of the choice of the substituents R at the 1,2-dithiolene core, allowing for the rational design of the linear and nonlinear optical properties of the resulting complexes, and hence to the possibility of applying them in fields as varied as nonlinear optics, photoconductivity, and electrochromism.

Further studies are ongoing in our laboratory to investigate in detail the role of the central metal ion and to generalize the limited findings described here for the Pd^{II} complexes with the mnt and Me_2timdt ligands to other homoleptic and heteroleptic bis(1,2-dithiolene) complexes differing for the nature of the central metal ions and 1,2-dithiolene ligands.

ASSOCIATED CONTENT

Supporting Information

The Supporting Information is available free of charge on the ACS Publications Web site at DOI: XXXX. Details on theoretical calculations. Molecular schemes for the compound discussed in the paper. Crystallographic data and packing details for complex **3**. Experimental UV–Vis–NIR spectra decomposed into their component Gaussian peaks. NIR spectra in MeCN, DMF, THF, CH_2Cl_2, and $CHCl_3$. KS frontier MO drawings calculated for Me_2timdt^{q-}, mnt^{q-} (q = 0, 1, 2), and complex **3**. RDFT, DFT-BS, and (IEF-PCM) TD-DFT data for **1** and **3**, calculated second-order hyperpolarizability β and dipole moments μ.

Accession Code

CCDC 2027023 contain the supplementary crystallographic data for this paper. These data can be obtained free of charge via www.ccdc.cam.ac.uk/data_request/cif, or by emailing data_request@ccdc.cam.ac.uk, or by contacting The Cambridge Crystallographic Data Centre, 12 Union Road, Cambridge CB2 1EZ, UK; fax: +44 1223 336033.

AUTHOR INFORMATION

Corresponding Authors

Massimiliano Arca – *Università degli Studi di Cagliari, Dipartimento di Scienze Chimiche e Geologiche, 09042 Monserrato (Cagliari), Italy; orcid.org/0000-0002-0058-6406; Email: marca@unica.it*

Anna Pintus – *Università degli Studi di Cagliari, Dipartimento di Scienze Chimiche e Geologiche, 09042 Monserrato (Cagliari), Italy; orcid.org/0000-0001-6069-9771; Email: apintus@unica.it*

Authors

M. Carla Aragoni – *Università degli Studi di Cagliari, Dipartimento di Scienze Chimiche e Geologiche, 09042 Monserrato (Cagliari), Italy; orcid.org/0000-0002-5010-7370*

Claudia Caltagirone – *Università degli Studi di Cagliari, Dipartimento di Scienze Chimiche e Geologiche, 09042 Monserrato (Cagliari), Italy; orcid.org/0000-0002-4302-0234*

Vito Lippolis – *Università degli Studi di Cagliari, Dipartimento di Scienze Chimiche e Geologiche, 09042 Monserrato (Cagliari), Italy; orcid.org/0000-0001-8093-576X*

Enrico Podda – *Università degli Studi di Cagliari, Dipartimento di Scienze Chimiche e Geologiche, 09042 Monserrato (Cagliari), Italy*

Alexandra M. Z. Slawin – *EaStCHEM School of Chemistry, University of St. Andrews, North Haugh, St. Andrews, Fife, KY16 9ST, UK*

J. Derek Woollins – *EaStCHEM School of Chemistry, University of St. Andrews, North Haugh, St. Andrews, Fife, KY16 9ST, UK and Department of Chemistry, Khalifa University, P.O. Box 127788, Abu Dhabi, United Arab Emirates.*

Author Contributions

The manuscript was written through contributions of all authors.

Notes

The authors declare no competing financial interest.

ACKNOWLEDGMENT

M. A., M. C. A., C. C., and V. L. thank the Fondazione di Sardegna (FdS) and Regione Autonoma della Sardegna (RAS) (Progetti Biennali di Ateneo FdS/RAS annualità 2018) for financial support. A.P. acknowledges RAS for the funding in the context of the POR FSE 2014–2020 (CUP F24J17000190009).

ABBREVIATIONS

BS, broken symmetry; CS, closed shell; DC, diradical character; GS, ground state; MO, molecular orbital; HOMO, highest occupied molecular orbital; KS, Kohn-Sham; LUMO, lowest unoccupied molecular orbital; NBMO, non-bonding molecular orbital; NLO, nonlinear optics; SONLO, second-order nonlinear optics.

REFERENCES

(1) McCleverty, J. A. Metal 1, 2-dithiolene and related complexes. *Prog. Inorg. Chem.* **1968**, *10*, 49–221.

(2) Mueller-Westerhoff, U. T.; Vance, B.; Yoon, D. I. The synthesis of Dithiolene Dyes with Strong Near-IR Absorption *Tetrahedron* **1980**, *47*, 909–932.

(3) Mueller-Westerhoff, U. T.; Vance, B. Dithiolenes and Related Species *Comprehensive Coordination Chemistry*, Pergamon Press, 2, Ch. 16.5, 595–631, 1987.

(4) Dithiolene Chemistry: Synthesis, Properties, and Applications; Stiefel, E. I., Ed.; Wiley: Hoboken, 2004.

(5) Gareau-de Bonneval, B.; Ching, K. I. M. C.; Alary, F.; Bui, T. T.; Valade, L. Neutral d^8 metal bis-dithiolene complexes: synthesis, electronic properties and applications. *Coord. Chem. Rev.* **2010**, *254*, 1457–1467.

(6) Arca, M.; Aragoni, M. C.; Pintus, A. in *Handbook of chalcogen chemistry;* Devillanova, F. A.; du Mont, W. –W., Eds.; RSC Publishing: Cambridge, 2013, pp 127–179.

(7) Robertson, N.; Cronin, L. Metal bis-1,2-dithiolene complexes in conducting or magnetic crystalline assemblies. *Coord. Chem. Rev.* **2002**, *227*, 93–127.

(8) Kobayashi, A.; Fujiwara, E.; Kobayashi, H. Single-Component Molecular Metals with Extended-TTF Dithiolate Ligands. *Chem. Rev.* **2004**, *104*, 5243–5264.

(9) Kato, R. Conducting metal dithiolene complexes: Structural and electronic properties. *Chem. Rev.* **2004**, *104*, 5319–5346.

(10) Faulmann, C.; Jacob, K.; Dorbes, S.; Lampert, S.; Malfant, I.; Doublet, M., –L.; Valade, L.; Real J. A. Electrical Conductivity and Spin Crossover: A New Achievement with a Metal Bis Dithiolene Complex *Inorg. Chem.* **2007**, *46*, *21*, 8548–8559.

(11) Nunes, J.; Figuera, M.; Belo, D.; Santos, I.; Ribeiro, B.; Lopes, E.; Heniriques, R.; Vidal-Gancedo, J.; Veciana, J.; Rovira, C.; Almeida, M. Transition Metal Bisdithiolene Complexes Based on Extended Ligands with Fused Tetrathiafulvalene and Thiophene Moieties: New Single-Component Molecular Metals. *Chem. – Eur. J.* **2007**, *13*, 9841–9849.

(12) Faulmann, C.; Cassoux, P. Solid-State Properties (Electronic, Magnetic, Optical) of Dithiolene Complex-Based Compounds *Progr. Inorg. Chem.* **2004**, 52, 399–489.

(13) Shen, W.-C.; Huo, P.; Huang, Y.-D.; Yin, J.-X.; Zhu, Q.-Y.; Dai, J. Photocurrent responsive films prepared from a nickel-dithiolate compound with directly bonded pyridyl groups. *RSC Adv.* **2014**, *4*, 60221–60226.

(14) Naito, T.; Karasudani, T.; Nagayama, N.; Ohara, K.; Konishi, K.; Mori, S.; Takano, T.; Takahashi, Y.; Inabe, T.; Kinose, S.; Nishihara, S.; Inoue,

K. Giant Photoconductivity in NMQ[Ni(dmit)$_2$]. *Eur. J. Inorg. Chem.* **2014**, 4000–4009.

(15) Dalgleish, S.; Matsushita, M. M.; Hu, L.; Li, B.; Yoshikawa, H.; Awaga, K. Utilizing photocurrent transients for dithiolene-based photodetection: stepwise improvements at communications relevant wavelengths. *J. Am. Chem. Soc.* **2012**, *134*, 12742–12750.

(16) Aragoni, M. C.; Arca, M.; Caironi, M.; Denotti, C.; Devillanova, F. A.; Grigiotti, E.; Isaia, F.; Laschi, F.; Lippolis, V.; Natali, D.; Pala, L.; Sampietro, M.; Zanello, P. Monoreduced [M(R,R'timdt)$_2$]$^-$ dithiolenes (M = Ni, Pd, Pt; R,R'timdt = disubstituted imidazolidine-2,4,5-trithione): solid state photoconducting properties in the third optical fiber window. *Chem. Commun.* **2004**, 1882–1883.

(17) Pintus, A.; Ambrosio, L.; Aragoni, M. C.; Binda, M.; Coles, S. J.; Hursthouse, M. B.; Isaia, F.; Lippolis, V.; Meloni, G.; Natali, D.; Orton, J. B.; Podda, E.; Sampietro, M.; Arca, M. Photoconducting Devices with Response in the Visible–Near-Infrared Region Based on Neutral Ni Complexes of Aryl-1,2-dithiolene Ligands, *Inorg. Chem.* **2020**, *59*, 6410–6421.

(18) Mueller-Westerhoff, U. T.; Vance, B.; Yoon, D. I. The synthesis of dithiolene dyes with strong near-IR absorption. *Tetrahedron* **1991**, *47*, 909–932.

(19) Liu, Y.; Zhang, Z.; Chen, X.; Xu, S.; Cao, S. Near-infrared absorbing dyes at 1064 nm: Soluble dithiolene nickel complexes with alkylated electron-donating groups as Peripheral substituents. *Dyes Pigm.* **2016**, *128*, 179–189.

(20) Chatzikyriatos, G.; Papagiannouli, I.; Couris, S.; Anyfantis, G. C.; Papavassiliou, G. C. Nonlinear optical response of a symmetrical Au dithiolene complex under ps and ns laser excitation in the infrared and in the visible. *Chem. Phys. Lett.* **2011**, *513*, 229–235.

(21) Guo, W. F.; Sun, X. B.; Sun, J.; Wang, X. Q.; Zhang, G. H.; Ren, Q.; Xu, D. Nonlinear optical absorption of a metal dithiolene complex irradiated by different laser pulses at near-infrared wavelengths. *Chem. Phys. Lett.* **2007**, *435*, 65–68.

(22) Cassano, T.; Tommasi, R.; Nitti, L.; Aragoni, M. C.; Arca, M.; Denotti, C.; Devillanova, F. A.; Isaia, F.; Lippolis, V.; Lelj, F.; Romaniello, P. Picosecond absorption saturation dynamics in neutral [M(R,R'timdt)$_2$] metal-dithiolenes. *J. Chem. Phys.* **2003**, *118*, 5995–6002.

(23) Arca, M.; Aragoni, M. C.; Pintus, A. in *Handbook of chalcogen chemistry;* Devillanova, F. A.; du Mont, W.-W., Eds.; RSC Publishing: Cambridge, 2013, pp 127–179.

(24) Barriere, F.; Camire, N.; Geiger, W. E.; Mueller-Westerhoof, U. T.; Sanders, R. Use of Medium Effects to Tune the $\Delta E_{1/2}$ Values of Bimetallic and Oligometallic Compounds. *J. Am. Chem. Soc.* **2002**, *124*, 7262–7263.

(25) Chirik, P. J. Preface: forum on redox-active ligands. *Inorg. Chem.* **2011**, *50*, 9737–9740.

(26) Eisenberg, R.; Gray, H. B. Electrochemical deposition of highly-conducting metal dithiolene films. *Inorg. Chem.* **2011**, *13*, 9841–9849.

(27) Eisenberg, R.; Gray, H. B. Noninnocence in metal complexes: A dithiolene dawn. *Inorg. Chem.* **2011**, *50*, 9741–9751.

(28) Periyasamy, G.; Burton, N. A.; Hillier, I. H.; Vincent, M. A.; Disley, H.; McMaster J.; Garner C. D. The dithiolene ligand--'innocent' or 'non-innocent'? A theoretical and experimental study of some cobalt-dithiolene complexes. *Faraday Discuss.* **2007**, *135*, 489–506.

(29) Lewis, G. R.; Dance I. Crystal supramolecular motifs for [Ph_4P]$^+$ salts of [M(mnt)$_2$]$^{2-}$, [M(mnt)$_2$]$^-$, [{M(mnt)$_2$}$_2$]$^{2-}$, [M(mnt)$_3$]$^{3-}$ and [M(mnt)$_3$]$^{2-}$ (mnt^{2-} = maleonitriledithiolate) *J. Chem. Soc., Dalton Trans.* **2000**, 3176–3185.

(30) Lim, B. S.; Fomitchev, D. V.; Holm R. H. Nickel Dithiolenes Revisited: Structures and Electron Distribution from Density Functional Theory for the Three-Member Electron-Transfer Series [Ni($S_2C_2Me_2$)$_2$]$^{0,1-,2-}$ *Inorg. Chem.* **2001,** *40,* 4257–4262.

(31) Madhu, V.; Das, S. K. New Series of Asymmetrically Substituted Bis(1,2-dithiolato)-Nickel (III) Complexes Exhibiting Near IR Absorption and Structural Diversity *Inorg. Chem.* **2008**, *47*, 5055–5070.

(32) Masui, H. Metalloaromaticity *Coord. Chem. Rev.* **2001**, *219–221*, 957–992.

(33) Ray, K.; Weyhermüller, T.; Neese, F.; Wieghardt, K. Electronic Structure of Square Planar Bis(benzene-1,2-dithiolato)metal Complexes [M(L)$_2$]^z (z = 2–, 1–, 0; M = Ni, Pd, Pt, Cu, Au): An Experimental, Density Functional, and Correlated ab Initio Study *Inorg. Chem.* **2005**, *44*, 5345–5360.

(34) Szilagyi, R. K.; Lim, B. S.; Glaser, T.;Holm, R. H.; Hedman, B.; Hodgson, K. O.; Solomon, E. I. Description of the Ground State Wave Functions of Ni Dithiolenes Using Sulfur K-edge X-ray Absorption Spectroscopy J. *Am. Chem. Soc.* **2003**, *125*, 9158–9169.

(35) Li, X. Y.; Sun, Y. G.; Huo, P.; Shao, M. Y.;Ji, S. F.; Zhu, Q. Y.; Dai, J. Metal centered oxidation or ligand centered oxidation of metal dithiolene? Spectral, electrochemical and structural studies on a nickel-4-pyridine-1,2-dithiolate system *Phys. Chem. Chem. Phys.* **2013**, *15*, 4016–4023.

(36) Ambrosio, L.; Aragoni, M. C.; Arca, M.; Devillanova, F. A.; Hursthouse, M. B.; Huth, S. L.; Isaia, F.; Lippolis, V.; Mancini, A.; Pintus, A. Synthesis and Characterization of Novel Gold (III) Complexes of Asymmetrically Aryl-Substituted 1,2-Dithiolene Ligands Featuring Potential-Controlled Spectroscopic Properties *Chem. – Asian J.* **2010**, 5, 1395–1406.

(37) Bachler, V.; Olbrich, G.; Neese, F.; Wieghardt, K. Theoretical evidence for the singlet diradical character of square planar nickel complexes containing two o-semiquinonato type ligands *Inorg. Chem.* **2002**, *41*, 4179–4193.

(38) Avramopoulos, A.; Reis, H.; G, Mousdis, Papadopoulos, M. G. Ni Dithiolenes – A Theoretical Study on Structure–Property Relationships *Eur. J. Inorg. Chem.* **2003**, 4839–4850.

(39) Avramopoulos, A.; Otero, N.; Reis, H.; Karamanis, P.; Papadopoulos, M. G. A computational study of photonic materials based on Ni bis(dithiolene) fused with benzene, possessing gigantic second hyperpolarizabilities *J. Mater. Chem. C* **2018**, *6*, 91–110.

(40) Dalgleish, S.; Robertson, N. A stable near IR switchable electrochromic polymer based on an indole-substituted nickel dithiolene *Chem. Commun.* **2009**, 5826–5828.

(41) Basu, P.; Nigam, A.; Mogesa, B.; Denti, S.; Nemykin, V. Synthesis, characterization, spectroscopy, electronic and redox properties of a new nickel dithiolene system *Inorg. Chim. Acta* **2010**, *363*, 2857–2864.

(42) Aragoni, M. C.; Arca, M.; Cassano, T.; Denotti, C.; Devillanova, F. A.; Isaia, F.; Lippolis, V.; Natali, D.; Nitti, L.; Sampietro, M.; Tommasi, R. Photoinduced conductivity and nonlinear optical properties of [M(R,R'timdt)$_2$] dithiolenes (M = Ni, Pd, Pt; R,R'timdt = monoreduced imidazolidine-2,4,5-trithione) as materials for optically driven switches and photodetectors *Inorg. Chem. Commun.* **2002**, *5*, 869–872.

(43) Natali, D.; Sampietro, M.; Arca, M.; Denotti, C.; Devillanova, F. A. Wavelenght selective photodetectors for Near-Infrared applications based on novel neutral dithiolenes *Synth. Metals* **2003**, *137*, 1489–1490.

(44) Caironi, M.; Natali, D.; Sampietro, M.; Ward, M.; Meacham, A.; Devillanova, F. A.; Arca, M.; Denotti, C.; Pala, L. Near-infrared detection by means of coordination complexes, *Synth. Metals* **2005**, *153*, 273–276.

(45) Arca, M.; Demartin, F.; Devillanova, F. A.; Garau, A.; Isaia, F.; Lelj, F.; Lippolis, V.; Pedraglio, S.; Verani, G. Synthesis, X-ray crystal structure and spectroscopic characterization of the new dithiolene [Pd(Et$_2$timdt)$_2$] and of its adduct with molecular diiodine [Pd(Et$_2$timdt)$_2$]·I_2·$CHCl_3$ (Et$_2$timdt = monoanion of 1,3-diethylimidazolidine-2,4,5-trithione) *J. Chem. Soc., Dalton Trans.* **1998**, 3731–3736.

(46) Aragoni, M.; Arca, M.; Demartin, F.; Devillanova, F. A.; Garau, A.; Isaia, F.; Lelj, F.; Lippolis, V.; Verani, G. New [M(R,R'timdt)$_2$] metal-dithiolenes and related compounds (M = Ni, Pd, Pt; R,R'timdt = monoanion of di-substituted imidazolidine-2,4,5-trithiones): an experimental and theoretical investigation *J. Am. Chem. Soc.* **1999**, *121*, 7098–7107.

(47) Cassano, T.; Tommasi, R.; Nitti, L.; Aragoni, M. C.; Arca, M.; Denotti, C.; Devillanova, F. A.; Isaia, F.; Lippolis, V.; Lelj, F.; Romaniello, P. Picosecond absorption saturation dynamics in neutral [M(R,R'timdt)$_2$] metal-dithiolenes *J. Chem. Phys.* **2003**, *118*, 5995–6002.

(48) Aragoni, M. C.; Arca, M.; Denotti, C.; Devillanova, F. A.; Grigiotti. E.; Isaia, F.; Laschi, F.; Lippolis, V.; Pala, L.; Slawin, A. M. Z.; Zanello, P.; Woollins, J. D. A facile synthesis via $[Pd(Et_2timdt)Br_2]$ of a push-pull mixed-ligand Pd-dithiolene containing the Et_2timdt ligand (Et_2timdt = diethylimidazolidine-2,4,5-trithione) *Eur. J. Inorg. Chem.* **2003**, *7*, 1291–1295.

(49) Aragoni, M. C.; Arca, M.; Cassano, T.; Denotti, C.; Devillanova, F. A.; Frau, R.; Isaia, F.; Lelj, F.; Lippolis, V.; Nitti, L.; Romaniello, P.; Tommasi, R.; Verani, G. NIR Dyes Based on $[M(R,R'timdt)_2]$ Metal-Dithiolenes: Additivity of M, R, and R' Contributions To Tune the NIR Absorption (M = Ni, Pd, Pt; R,R'timdt = Monoreduced Form of Disubstituted Imidazolidine-2,4,5-trithione), *Eur. J. Inorg. Chem*. **2003**, 1939–1947.

(50) Aragoni, M. C.; Arca, M.; Demartin, F.; Devillanova, F. A.; Lelj, F.; Isaia, F.; Lippolis, V.; Mancini, A.; Pala, L.; Verani, G. A theoretical investigation of the donor ability of $[M(R,R'timdt)_2]$ dithiolenes towards molecular diiodine (M = Ni, Pd, Pt; R,R'timdt = formally monoreduced disubstituted imidazolidine-2,4,5-trithione) *Eur. J. Inorg. Chem.* **2004**, 3099–3109.

(51) Aragoni, M.; Arca, M.; Caironi, M.; Denotti, C.; Devillanova, F. A.; Grigiotti, E.; Isaia, F.; Laschi, F.; Lippolis, V.; Natali, D.; Pala, L.; Sampietro, M.; Zanello, P. Monoreduced $[M(R,R'timdt)_2]^-$ dithiolenes: solid state photoconducting properties in the third optical fiber window, *Chem. Commun.* **2004**, 1882–1883.

(52) Deiana, C.; Aragoni, M. C.; Isaia, F.; Lippolis, V.; Pintus, A.; Slawin, A. M. Z.; Woollins, J. D.; Arca, M. Structural tailoring of the NIR-absorption of bis(1,2-dichalcogenolene) Ni/Pt electrochromophores deriving from 1,3-dimethyl-2-chalcogenoxo-imidazoline-4,5-dichalcogenolato, *New J. Chem.* **2016**, *40*, 8206–8210.

(53) Ahmadi, M.; Fischer, C.; Ghosh, A. C.; Schultze, C. An Asymmetrically Substituted Aliphatic Bis-Dithiolene Mono-Oxido Molybdenum (IV) Complex With Ester and Alcohol Functions as Structural and Functional Active Site Model of Molybdoenzymes *Front. Chem.* **2019**, *7*, article 486, 1–14.

(54) Chen, C. –T.; Liao, S. –Y.; Lin, K. –J.; Lai, L. –L. Syntheses, Charge Distribution, and Molecular Second-Order Nonlinear Optical Properties of Push–Pull Bisdithiolene Nickel Complexes *Adv. Mater*. **1998**, *3*, 334–338.

(55) Chen, X. -R.; Xue, C.; Liu, S. -X.; Cai, B.; Wang, Y.; T. J. -Q.; Xue, Y. -S.; Huang, X. -C.; Ren, X. -M.; Liu, J. -L. Investigation on crystal structure, magnetic and near-infrared absorption properties of a novel heteroleptic nickel-bis-1,2-dithiolene compound, Polyhedron **2017**, *132*, 12–19.

(56) Obanda, A.; Martinez, K.; Schmehl, R. H.; Mague, J. T.; Rubtson, I. V.; MacMillan, S. N.; Lancaster, K. M.; Sproules, S.; Donahue, J. P. Expanding the Scope of Ligand Substitution from $[M(S_2C_2Ph_2]$ (M = Ni^{2+}, Pd^{2+}, Pt^{2+}) To Afford New Heteroleptic Dithiolene Complexes *Inorg. Chem*. **2017**, *56*, 10257–10267.

(57) A search on the Cambridge structural database for heteroleptic bis(1,2-dithiolene) metal complexes $[M(\mathbf{L})(\mathbf{L}')]$ shows 33 examples for M = Ni and only 7 with M = Pd. Among these 40 complexes, 9 show the mnt ligand.

(58) Jeannin, O.; Delaunay, J.; Barrière, F.; Fourmigué, M. Between $Ni(mnt)_2$ and $Ni(tfd)_2$ Dithiolene Complexes: the Unsymmetrical 2-(Trifluoromethyl)acrylonitrile-1,2-dithiolate and Its Nickel Complexes *Inorg. Chem.* **2005**, *44*, 9763–9770.

(59) Papavassiliou, G. C.; Anyfantis, G. C.; Mousdis, G. A. Neutral Metal 1,2-Dithiolenes: Preparations, Properties and Possible Applications of Unsymmetrical in Comparison to the Symmetrical *Crystals* **2012**, *2*, 762–811.

(60) Anyfantis, G. C.; Papavassiliou, G. C.; Aloukos, P.; Couris, S.; Weng, Y. F.; Yoshino, Harukazu; Murata, K. Unsymmetrical Single-Component Nickel 1,2-Dithiolene Complexes with Extended Tetrachalcogenafulvalenedithiolato Ligands *Z. Naturforsch.* **2007**, *62b*, 200–204.

(61) Papavassiliou, G. C.; Anyfantis, G. C.; Steele, B. R.; Terzis, A.; Raptopoulou, C. P.; Tatakis, G.; Chaidogiannos, G.; Glezos, N.; Weng, Y.; Yoshino, H.; Murata, K. Some New Nickel 1,2-Dichalcogenolene Complexes as Single-component Semiconductors *Z. Naturforsch.* **2007**, *62b*, 679–684.

(62) Pintus, A.; Aragoni, M. C.; Bellec, N.; Devillanova, F. A.; Lorcy, D.; Isaia, F.; Lippolis, V.; Randall, R. A. M.; Roisnel, T.; Slawin, A. M. Z.; Woollins, J. D.; Arca M. Structure–Property Relationships in Pt^{II} Diimine-Dithiolate Nonlinear Optical Chromophores Based on Arylethylene-1,2-dithiolate and 2-Thioxothiazoline-4,5-dithiolate *Eur. J. Inorg. Chem.* **2012**, 3577–3594.

(63) Pintus, A.; Aragoni, M. C.; Coles, S. J.; Coles, S. L.; Isaia, F.; Lippolis, V.; Musteti, A. -D.; Teixidor, F.; Viñas, C.; Arca, M. New Pt^{II} diimine-dithiolate complexes containing a 1,2-dithiolate-1,2-closo-dicarbadodecarborane: an experimental and theoretical investigation *Dalton Trans.* **2014**, *43*, 13649–13660.

(64) Pintus, A.; Aragoni, M. C.; Isaia, F.; Lippolis, V.; Lorcy, D.; Slawin, A. M. Z.; Woollins, J. D.; Arca, M. On the Role of Chalcogen Donor Atoms in Diimine-Dichalcogenolate Pt^{II} SONLO Chromophores: Is It Worth Replacing Sulfur with Selenium? *Eur. J. Inorg. Chem.* **2015**, 5163–5170.

(65) Aragoni, M. C.; Arca, M.; Crisponi, G. Nurchi, V. M. Simultaneous decomposition of several spectra into the constituent Gaussian peaks, *Anal. Chim. Acta* **1995**, *316*, 195–204.

(66) Wojdyr, M. Fityk: a general-purpose peak fitting program *J. Appl. Cryst.* **2010**, *43*, 1126–1128.

(67) Bruno, I. J.; Cole, J. C.; Edgington, P. R.; Kessler, M.; Macrae, C. F.; McCabe, P.; Pearson, J.; Taylor, R. New software for searching the Cambridge Structural Database and visualizing crystal structures *Acta Cryst. B* **2002**, *58*, 389–397.

(68) Sheldrick, G. M.; *SHELXS-97*, Program for Crystal Structure Solution; University of Göttingen: Gottingen, Germany, 1997.

(69) Sheldrick, G. M.; *SHELXL-97*, Program for X-ray Crystal Structure Refinement; University of Göttingen: Germany, 1997.

(70) Arca, M.; Demartin, F.; Devillanova, F. A.; Isaia, F.; Lelj, F.; Lippolis, V.; Verani, G. An experimental and theoretical approach to the study of the properties of parabanic acid and related compounds: synthesis and crystal structure of diethylimidazolidine-2-selone-4,5- dione *Can. J. Chem*. **2000**, *78*, 1147–1157.

(71) Cummings, S. D.; Cheng, L.-T.; Eisenberg, R. Metalloorganic Compounds for Nonlinear Optics: Molecular Hyperpolarizabilities of M(diimine)(dithiolate) Complexes (M = Pt, Pd, Ni) *Chem. Mater.* **1997**, *9*, 440–450.

(72) Wang, Y.; Hickox, H. P.; Xie, Y.; Wei, P.; Blair, S. A.; Johnson, M. K.; Schaefer, H. F. III; Robinson, G. H. A Stable Anionic Dithiolene Radical *J. Am. Chem. Soc.* **2017**, *139*, 6859–6862.

(73) Wang, Y.; Xie, Y.; Wei, P.; Blair, S. A.; Cui, D.; Johnson, M. K.; Schaefer, H. F. III; Robinson, G. H. Stable Boron Dithiolene Radicals *Angew. Chem. Int. Ed*. **2018**, *57*, 7865–7868.

(74) Karthik, V.; Bhat, I. A.; Anantharaman, G. Backbone Thio-Functionalized Imidazol-2-ylidene–Metal Complexes: Synthesis, Structure, Electronic Properties, and Catalytic Activity *Organomet.* **2013**, *32*, 7006–7013.

(75) Koch, W.; Holthausen, M. C. *A Chemist's Guide to Density Functional Theory*, Wiley-VCH: Weinheim, 2nd edn, 2002.

(76) Frisch, M. J.; Trucks, G. W.; Schlegel, H. B.; Scuseria, G. E.; Robb, M. A.; Cheeseman, J. R.; Scalmani, G.; Barone, V.; Petersson, G. A.; Nakatsuji, H.; Li, X.; Caricato, M.; Marenich, A. V.; Bloino, J.; Janesko, B. G.; Gomperts, R.; Mennucci, B.; Hratchian, H. P.; Ortiz, J. V.; Izmaylov, A. F.; Sonnenberg, J. L.; Williams-Young, D.; Ding, F.; Lipparini, F.; Egidi, F.; Goings, J.; Peng, B.; Petrone, A.; Henderson, T.; Ranasinghe, D.; Zakrzewski, V. G.; Gao, J.; Rega, N.; Zheng, G.; Liang, W.; Hada, M.; Ehara, M.; Toyota, K.; Fukuda, R.; Hasegawa, J.; Ishida, M.; Nakajima, T.; Honda, Y.; Kitao, O.; Nakai, H.; Vreven, T.; Throssell, K.; Montgomery, J. A. Jr.; Peralta, J. E.; Ogliaro, F.; Bearpark, M. J.; Heyd, J. J.; Brothers, E. N.; Kudin, K. N.; Staroverov, V. N.; Keith, T. A.; Kobayashi, R.; Normand, J.; Raghavachari, K.; Rendell, A. P.; Burant, J. C.; Iyengar, S. S.; Tomasi, J.; Cossi, M.; Millam, J. M.; Klene, M.; Adamo, C.; Cammi, R.; Ochterski, J. W.; Martin, R. L.; Morokuma, K.; Farkas, O.; Foresman, J. B.; Fox, D. J.; *Gaussian 16, Revision B.01*; Gaussian, Inc.: Wallingford CT, 2016

(77) Becke, A. D. Density-functional thermochemistry. III. The role of exact exchange *J. Chem. Phys.* **1993**, *98*, 5648–5652.

(78) Adamo, C., Barone, V. Exchange functionals with improved long-range behavior and adiabatic connection methods without adjustable parameters: The mPW and mPW1PW models *J. Chem. Phys.* **1998**, *108*, 664–675.

(79) Adamo, C.; Barone, V. Toward reliable density functional methods without adjustable parameters: The PBE0 model *J. Chem. Phys.* **1999**, *110*, 6158–6170.

(80) Dunning, T. H. Jr.; Hay P. J. in "Methods of Electronic Structure, Theory", Vol. 2, H. F. Schaefer III ed., Plenum Press, **1977**.

(81) Ortiz, J. V.; Hay, P. J.; Martin, R. L. Role of d and f orbitals in the geometries of low-valent actinide compounds *J. Am. Chem. Soc.* **1992**, *114*, 2736–2737.

(82) Roy, L. E.; Hay, P. J;. Martin, R. L. Revised Basis Sets for the LANL Effective Core Potentials *J. Chem. Theor. Comp*. **2008**, *4*, 1029–1031.

(83) Stevens, W. J.; Krauss, M.; Basch, H.; Jasien, P. G. Relativistic compact effective potentials and efficient, shared- exponent basis sets for the third-, fourth-, and fifth row atoms *Can. J. Chem.* **1992**, *70*, 612–630.

(84) Kaupp, M.; Schleyer, P. V. R.; Stoll, H.; Preuss, H. Pseudopotential approaches to Ca, Sr, and Ba hydrides. Why are some alkaline earth MX2 compounds bent? *J. Chem. Phys.* **1991**, *94*, 1360–1366.

(85) Ermler, W. C.; Ross, R. B.; Christiansen, P. A. Ab initio relativistic effective potentials with spin-orbit operators. VI. Fr through Pu *Int. J. Quant. Chem.* **1991**, *40*, 829–846.

(86) Wadt, W. R.; Hay, P. J. Ab initio effective core potentials for molecular calculations. Potentials for the transition metal atoms Sc to Hg *J. Chem. Phys.*, **1985**, *82*, 270–283; *ibid.* 284–298; *ibid.* 299–310.

(87)Perdew, J. P.; Chevary, J. A.; Vosko, S. H.; Jackson, K. A.; Pederson, M. R.; Singh, D. J.; Fiolhais, C. Atoms, molecules, solids, and surfaces: Applications of the generalized gradient approximation for exchange and correlation *Phys. Rev. B* **1992**, *46*, 6671–6687.

(88) Perdew, J. P.; Chevary, J. A.; Vosko, S. H.; Jackson, K. A.; Pederson, M. R.; Singh, D. J.; Fiolhais, C. Atoms, molecules, solids, and surfaces: Applications of the generalized gradient approximation for exchange and correlation *Phys. Rev. B* **1993**, *48*, 4978–4978.

(89) Schäfer, A.; Horn, H.; Ahlrichs, R. Fully optimized contracted Gaussian basis sets for atoms Li to Kr. *J. Chem. Phys.* **1992**, *97*, 2571–2577.

(90)Pritchard, B. P.; Altarawy, D.; Didier, B.; Gibson, T. D.; Windus T. L. A New Basis Set Exchange: An Open, Up-to-date Resource for the Molecular Sciences Community *J. Chem. Inf. Model.* **2019**, *59*, 4814–4820.

(91) Abe, M. Diradicals *Chem. Rev.* **2013**, *113*, 7011–7088.

(92)Srinivas, K.; Prabhakar, Ch.; Lavanya Devi, C.; Yesudas, K.; Bhanuprakash, K.; Jayathirtha Rao, V. Enhanced Diradical Nature in Oxyallyl Derivatives Leads to Near Infra Red Absorption: A Comparative Study of the Squaraine and Croconate Dyes Using Computational Techniques *J. Phys. Chem. A* **2007**, *111*, 3378–3386.

(93) Mostafanejad, M. Basics of the Spin Hamiltonian Formalism *Int. J. Quantum Chem.* **2014**, *114*, 1495–1512.

(94) Bendikov, M.; Duong, H. M.; Starkey, K.; Houk, K. N.; Carter, E. A.; Wudl, F., Oligoacenes: Theoretical Prediction of Open-Shell Singlet Diradical Ground States *J. Am. Chem. Soc.* **2004**, *126*, 7416–7417.

(95) Schmidt, J. R.; Shenvi, N.; Tully, J. C. Controlling spin contamination using constrained density functional theory *J. Chem. Phys.* **2008**, *129*, 114110-1–10.

(96) Reed, A. E.; Weinstock, R. B.; Weinhold, F. Natural population analysis. *J. Chem. Phys*. **1985**, *83*, 735–746.

(97) Wiberg, K. B. Application of the pople-santry-segal CNDO method to the cyclopropylcarbinyl and cyclobutyl cation and to bicyclobutane *Tetrahedron* **1968**, *24*, 1083–1096.

(98) Adamo C.; Jacquemin D. The calculations of excited-state properties with Time-Dependent Density Functional Theory *Chem. Soc. Rev.* **2013**, *42*, 845–856.

(99) Laurent, A. D.; Jacquemin D. TD-DFT benchmarks: A review *Int. J. Quantum Chem.* **2020**, *113*, 2019–2039.

(100) Tomasi, J.; Mennucci, B.; Cammi, R. Quantum mechanical continuum solvation models. *Chem. Rev.* **2005**, *105*, 2999–3094.

(101) Jodaian, V.; Mirzaei, M.; Arca, M.; Aragoni, M. C.; Lippolis, V.; Tavakoli, E.; Langeroodi, N. S. First example of a 1:1 vanadium(IV)–citrate complex featuring the 2,2′-bipyridine co-ligand: Synthesis, X-ray crystal structure and DFT calculations *Inorg. Chim. Acta* **2013**, *400*, 107–114.

(102) Day, P. N.; Nguyen, K. A.; Pachter, TDDFT Study of One- and Two-Photon Absorption Properties: Donor–π–Acceptor Chromophores R. *Chem. Phys. B* **2005**, *109*, 1803–1814.

(103) Huong, V. T. T.; Tai, T. B.; Nguien, M. T. A theoretical study on charge transport of dithiolene nickel complexes *Phys. Chem. Chem. Phys.* **2016**, *18*, 6259–6267.

(104) Davis, A. P.; Fry, A. J. Experimental and computed absolute redox potentials of polycyclic aromatic hydrocarbons are highly linearly correlated over a wide range of structures and potentials *J. Phys. Chem. A* **2010**, *114*, 12299–12304.

(105) Yan, L.; Lu, Y.; Li, X. A density functional theory protocol for the calculation of redox potentials of copper complexes *Phys. Chem. Chem. Phys.* **2016**, *18*, 5529–5536.

(106) Baik, M. –H.; Friesnel, R. A. Computing Redox Potentials in Solution: Density Functional Theory as A Tool for Rational Design of Redox Agents *J. Phys. Chem. A* **2002**, *106*, 7407–7412.

(107) Bartmess, J. E. Thermodynamics of the Electron and the Proton *J. Phys. Chem.* **1994**, *98*, 6420–6424.

(108) Jiang, S.; Xu, M. Hyperpolarizabilities for the one-dimensional infinite single-electron periodic systems. I. Analytical solutions under dipole-dipole correlations *J. Chem. Phys.* **2005**, *123*, 064901-1–12.

(109) Cifuentes, M. P.; Humphrey, M. G. Alkynyl compounds and nonlinear optics *J. Organomet. Chem.* **2004**, 3968–3981.

(110) Mendes, P. J.; Carvalho, A. J. P.; Ramalho, J. P. P. Role played by the organometallic fragment on the first hyperpolarizability of iron–acetylide complexes: A TD-DFT study *J. Mol. Struct.: THEOCHEM* **2009**, *900*, 110–117.

(111) Schaftenaar, G.; Noordik, J. H. Molden: a pre-and post-processing program for molecular and electronic structures. *J. Comput. – Aided Mol. Des.* **2000**, *14*, 123–134.

(112) Dennington, R.; Keith, T. A.; Millam, J. M.; *GaussView, Version 6*; Semichem Inc.: Shawnee Mission, KS, 2016.

(113) O'Boyle, N. M.; Tenderholt, A. L.; Langner, K. M. Clib: a library for package-independent computational chemistry algorithms. *J. Comput. Chem.* **2008**, *29*, 839–845.

(114) Chemissian, a computer program to analyze and visualize quantum-chemical calculations written by L. Skripnikov. For the current version, see http://www.chemissian.com.

(115) Scheibye, S.; Pedersen, B. S.; Lawesson, S.-O. Studies on organophosphorus compounds XXI. The dimer of p-methoxyphenylthionophosphine sulfide as thiation reagent. A new route to thiocarboxamides *Bull. Soc. Chim. Belg*. **1978**, *87*, 229–238.

(116) Domingos, A.; Henriques, R. T.; Gama, V.; Almeida, M.; Lopes Vieira, A.; Alcacer, L. Crystalline structure/transport properties relationship in the (perylene)$_2$M(mnt)$_2$ family M=Au, Pd, Pt, Ni) *Synth. Met.* **1988**, *27*, 411–416.

(117) Average value calculated on 13 structures deposited at the CCDC and featuring a $[Pd(mnt)_2]^-$ anion (JUJGOK, JUJGOK, JUJGOK01, JUJGOK01, KOJTUY, MOSXID, SAHFEM, SAMCIT, SAMCIT, SATVAK, SICFOB, UCUHIK, WAPBAS).

(118) Average value calculated on 21 structures deposited at the CCDC and featuring a $[Pd(mnt)_2]^{2-}$ anion (LEHFOU, PAZSIT, BAHMOO, BUTSUF, CAJQEM, EBOZEB, HAVYOT, ICUBIS, JUJGIE, JUJGIE01, MOQCIF, NALTEZ, OPAMAU, VUQWOU, WABDIN, WASKUW, YICKUR, YOBMEH, KANZOQ, SAHFOW, XOJXAX).

(119) Damas, A.; Chamereau, L. –M.; Cooksy, A. L.; Jutand, A.; Amouri, H. π-Bonded Dithiolene Complexes: Synthesis, Molecular Structures, Electrochemical Behavior, and Density Functional Theory Calculations *Inorg. Chem.* **2013**, *52*, 1409–1417.

(120) Hencher, J. L.; Shen, Q.; Tuck, D, G. Molecular structure of 1,2-bis(trifluoromethyl)dithiete by vapor phase electron diffraction *J. Am. Chem. Soc.* **1976**, *98*, 899–902.

(121) Shimizu, T.; Murakami, H.; Kobayashi, Y.; Iwata, K.; Kamigata, N. Synthesis, Structure, and Ring Conversion of 1,2-Dithiete and Related Compounds *J. Org. Chem.* **1998**, *63*, 8192–8199.

(122) Donahue, J. P.; Holm, R. H. 3,4-Bis(1-adamantyl)-1,2-dithiete: the First Structurally Characterized Dithiete Unsupported by a Ring or Benzenoid Frame *Acta Cryst. C* **1998**, *54*, 1175–1178.

(123) Roesky, H.W.; Hofmann, H.; Clegg, W.; Noltemeyer, M.; Sheldrick, G. M. Preparation and crystal structure of cyclic dithiooxamides *Inorg. Chem.* **1982**, *21*, 3798–3800.

(124) Aragoni, M. C.; Arca, M.; Devillanova, F. A.; Isaia, F.; Lippolis, V.; Mancini, A.; Pala, L.; Slawin, A. M. Z.; Woollins, J. D. First example of infinite polybromide 2D network *Chem. Commun.* **2003**, 2226–2227.

(125) Davis, A. P.; Fry, A. J. Experimental and computed absolute redox potentials of polycyclic aromatic hydrocarbons are highly linearly correlated over a wide range of structures and potentials *J. Phys. Chem. A* **2010**, *114*, 12299–12304.

(126) Baik, M. –H.; Friesnel, R. A. Computing Redox Potentials in Solution: Density Functional Theory as A Tool for Rational Design of Redox Agents *J. Phys. Chem. A* **2002**, *106*, 7407–7412.

(127) Canola, S.; Casado, J. Negri, F. The double exciton state of conjugated chromophores with strong diradical character: insights from TDDFT calculations *Phys. Chem- Chem. Phys.* 2018, 20, 24227–24238.

(128) Wirz, J. Spectroscopic and kinetic investigations of conjugated biradical intermediates *Pure & Appl. Chem.* **1984**, *56(9)*, 1289–1300.

(129) Evangelista, F. A.; Allen, W. D.; Schaefer, H. F., III. Coupling term derivation and general implementation of state-specific multireference coupled cluster theories *J. Chem. Phys.* **2007**, *127*, 024102-1–17.

(130) Matsumoto, M.; Antol, I.; Abe, M. Curve Effect on Singlet Diradical Contribution in Kekulé-type Diradicals: A Sensitive Probe for Quinoidal Structure in Curved π-Conjugated Molecules **2019**, *24*, 209; doi:10.3390/molecules24010209.

(131) Noodleman, L. J. Valence bond description of antiferromagnetic coupling in transition metal dimers *Chem. Phys.* **1981**, *74*, 5737–5743.

(132) Noodleman, L.; Baerends, E. J. Electronic structure, magnetic properties, ESR, and optical spectra for 2-iron ferredoxin models by LCAO-Xα valence bond theory *J. Am. Chem. Soc.* **1984**, *106*, 2316–2327.

(133) Yamaguchi, K.; Takahara, Y.; Fueno, T.; Nasu, K. Ab Initio MO Calculations of Effective Exchange Integrals between Transition-Metal Ions via Oxygen Dianions: Nature of the Copper-Oxygen Bonds and Superconductivity *Jpn. J. Appl. Phys.* **1987**, *26*, L1362–L1364.

(134) Yamaguchi, K.; Jensen, F.; Dorigo, A.; Houk, K. N. A spin correction procedure for unrestricted Hartree-Fock and Møller-Plesset wavefunctions for singlet diradicals and polyradicals *Chem. Phys. Lett.* **1988**, *149*, 537–542.

(135) Malrieu, J. –P.; Trinquier, G. Communication: Proper use of broken-symmetry calculations in antiferromagnetic polyradicals *J. Chem. Phys.* **2016**, *144*, 211101-1–4.

(136) D. C. Young, Ch. 27 in "Computational Chemistry: A Practical Guide for Applying Techniques to Real-World Problems", J. Wiley and Sons, 2001, ISBN: 0-471-33368-9.

(137) CSD codes: BAHMOO, BUTSUF, CAJQEM„EBOZEB, HAVYOT, ICUBIS, JUJGIE, JUJGIE01, JUJGOK, JUJGOK01, KANZOQ, MOQCIF, MOSXID, NALTEZ, OPAMAU, SAHFEM, SAHFOW, SAMCIT, SATVAK, SICFOB, TENVIU, TENVOA, TENVUG, TEPCUP, TUKYAZ, UCUHIK, VUQWOU, WABDIN, WAPBAS, WASKUW, XOJXAX, YICKUR, YOBMEH, YOFCEB.

(138) Schulten, K.; Karplus, M. A low-lying weak transition in the polyene α,ω-diphenyloctatetraene *Chem. Phys. Lett.* **1972**, *14*, 299–304.

(139) Schulten, K.; Karplus, M. On the origin of low-lying forbidden transition in polyenes and related molecules *Chem. Phys. Lett.* **1972**, *14*, 305–309.

(140) Di Motta, S.; Negri, F.; Fazzi, D.; Castiglioni, C.; Canesi, E. V. Biradicaloid and Polyenic Character of Quinoidal Oligothiophenes Revealed by the Presence of a Low-Lying Double-Exciton State *J. Phys. Chem. Lett.* **2010**, *1*, 3334–3339.

(141) For the sake of comparison, calculations were repeated by adopting the B3LYP hybrid functional, including a 20% HF exchange, in place of mPW1PW (25% HF exchange). The corresponding DC index was n_{DC}= 17.4%.